AD NUMBER

AD853068

NEW LIMITATION CHANGE

TO

Approved for public release, distribution unlimited

FROM

Distribution authorized to U.S. Gov't. agencies and their contractors; Operational and Administrative Use; Mar 1969. Other requests shall be referred to Air Force Institute of Technology, School of Engineering, Wright-Patterson AFB, OH 45433.

AUTHORITY

DoDD 5230.24, 18 Mar 1987

AIR FORCE INSTITUTE OF TECHNOLOGY

AIR UNIVERSITY
UNITED STATES AIR FORCE

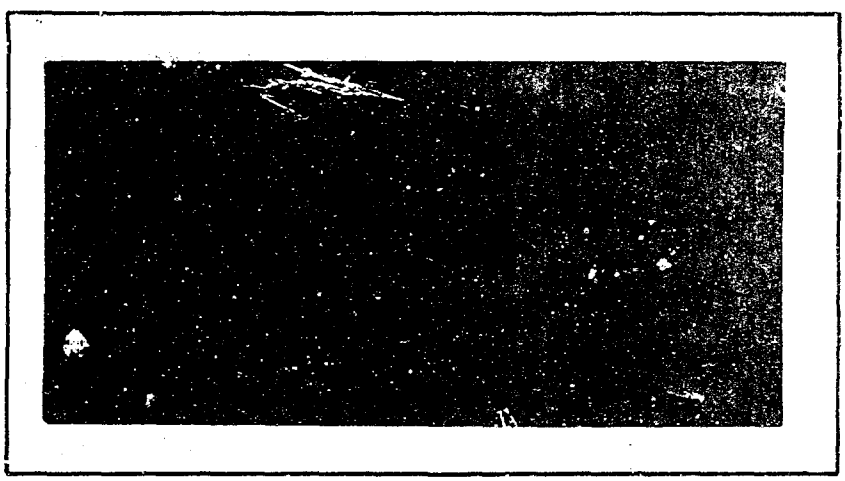

SCHOOL OF ENGINEERING

WRIGHT-PATTERSON AIR FORCE BASE, OHIO

59

INTERFEROMETER STUDY OF FREE CONVECTION ABOUT A RECTANGULAR CAVITY IN A FLAT PLATE

THESIS

Karl E. Luesse
GAM/ME/69-10 1/Lt USAF

AFLC-WPAFB-APR 69 35

INTERFEROMETER STUDY OF FREE CONVECTION ABOUT A RECTANGULAR CAVITY IN A FLAT PLATE

THESIS

Presented to the Faculty of the School of Engineering of

the Air Force Institute of Technology

Air University

in Partial Fulfillment of the

Requirements for the Degree of

Master of Science

by

Karl E. Luesse, B.S.M.E.

1/Lt USAF

Graduate Aerospace-Mechanical Engineering

March 1969

Preface

In this report I have attempted to describe an experimental study conducted to determine the effect of a rectangular cavity on the free convection heat transfer rate from a heated vertical flat plate. It was my intention that the flow over this plate be turbulent, but the flow went from laminar to turbulent with a third of the flow being in the transition phase. The Grashof number ranged from 1.75×10^9 to 1.24×10^{10}. The cavities studied had depths of 0.2 in, 0.4 in, and 0.6 in, and all had a width of 1.0 in. The plate to ambient temperature difference ($T_p - T_a$) was constant at 130 R and the pressure was atmospheric.

I wish to express my sincere appreciation to Dr. Andrew J. Shine who constantly showed a personal interest in my study and was always willing to give me advice while giving the same personal and knowledgeable advice to eight other graduate students.

I would like to gratefully acknowledge the help of Messrs. Bill Baker, Dick Brown, and especially John Flahive. Mr. Millard Wolf, supervisor of the school shops, is thanked for his assistance. I wish to thank the Whitley family, my neighbors, who edited and proof read each section of this report. Extra thanks go to Sgt. Whitley's son, Robert, whose help was most appreciated.

Finally I wish to thank my wife, Josephine, for her untiring assistance and her patience with an often irritable husband. I thank all the previously mentioned individuals but accept full responsibility for the material contained herein.

Karl E. Luesse

Contents

List of Figures

List of Symbols and Subscripts

Symbol	Quantity	Unit
A	Area	ft^2
b	Cavity width	in
d	Cavity depth	in
g_c	Dimensional conversion constant	ft lb_m/sec^2 lb_f
Gr	Grashof number	
h	Heat transfer coefficient	B/hr ft^2 R
k	Thermal conductivity	B/hr ft R
n	Fringe numbers (fringe 1 next to plate)	
Nu	Nusselt number	
Pr	Prandtl number	
q	Heat transfer rate	B/hr ft^2
s	Total number of fringes	
T	Absolute temperature	R
$\left(\frac{\partial T}{\partial y}\right)_p$	Temperature gradient at plate	R/ft
W	Test plate width	ft
x	Distance measured vertically from leading edge of plate (elevation)	in
y	Distance measured normal to plate surface	in
β	Coefficient of expansion	1/R
η	Refractive index of air	
θ	Difference between plate and ambient temperatures	R
λ	Wavelength of filtered interferometer light source	Angstrom
ρ	Density	lb_m/ft^3

Subscripts

a	Ambient air conditions
0	Standard conditions of temperature (OC) and pressure (29.92 in Hg)
f	Smooth flat plate
p	Plate
x	Position along plate

Abstract

The effect of a rectangular cavity on the free convection heat transfer rate from a vertical heated flat plate was experimentally studied. A Mach-Zehnder interferometer was used to obtain the temperature gradient at the plate surface. A series of tests with a smooth flat plate was made to establish a reference. A single cavity 1 in wide with depths of 0.2 in, 0.4 in, and 0.6 in was placed perpendicular to the flow. This cavity was located at four different elevations (distance from leading edge) 26.7 in, 32.7 in, 38.7 in, and 44.7 in. The plate to ambient temperature difference was maintained at 130 R. The range of Grashof numbers for this study was 1.75×10^9 to 1.24×10^{10}.

It was determined that the boundary layer went from laminar to turbulent with one third of the flow studied being in the transition phase. The effect of the cavity on the heat transfer rate varied depending on the type of flow (degree of turbulence or Grashof number). The maximum increase in the heat transfer rate (40%) occurred in the laminar region with the cavity at an elevation of 26.7 in. The maximum decrease in the heat transfer rate (25%) occurred in the turbulent region with the cavity at an elevation of 44.7 in.

INTERFEROMETER STUDY OF FREE CONVECTION ABOUT A RECTANGULAR CAVITY IN A FLAT PLATE

I. Introduction

This study was an out-growth of the work of Fletcher (Ref 7). Fletcher studied the effect of various rectangular cavities on the free convection heat transfer rate from a vertical flat plate to a laminar boundary layer. In that study the Grashof numbers at the various cavity locations were: 8.4×10^6, 4.7×10^7, 2.8×10^8. Fletcher showed a net increase in the heat transfer rate from 3.1% to 8.6% (based on locally affected area). There are several studies which show the effect of a rectangular cavity on the heat transfer rate in turbulent forced convection (Refs 2,6,8). Chapman (Ref 2) found that the average heat transfer coefficient of the cavity was only 56% of that of a flat plate.

The object of this study was to obtain data on the free convection heat transfer rate from a heated vertical flat plate to a turbulent boundary layer and compare the results with those of Fletcher. There is no universally accepted value of the Grashof number above which the flow can be considered to be turbulent. Eckert and Soehngen (Ref 5:2) stated that transition to turbulence began at $Gr = 4\times10^8$. Bayley (Ref 1:4) determined the transition point to be $Gr\times Pr = 2\times10^9$ or $Gr = 2.86\times10^9$. Cheeswright (Ref 3:1) determined that transition

occurred between Gr = 2×10^9 and Gr = 10^{10}. To obtain a turbulent boundary layer, the heated plate for this study was designed to give a Grashof number range of 1.75×10^9 to 1.24×10^{10}. This was obtained by designing a plate 50 in long and by maintaining a temperature difference of 130 R between the plate surface and the ambient air. The cavity was milled across the 8 in width of the plate; it was 1 in wide in the vertical direction; and its depth was varied in three increments to 0.2 in, 0.4 in, and 0.6 in. The cavity was placed at four different elevations (26.7 in, 32.7 in, 38.7 in, 44.7 in) along the plate.

II. Apparatus

The apparatus used in this investigation was basically the same as that of Fletcher (Ref 7). The major difference between that of Fletcher and that of this study was the addition of a 26 in long leading edge to make the plate long enough to obtain a turbulent flow. Figure 1 is a view of the experimental set-up. A more detailed presentation of apparatus is contained in Appendix B.

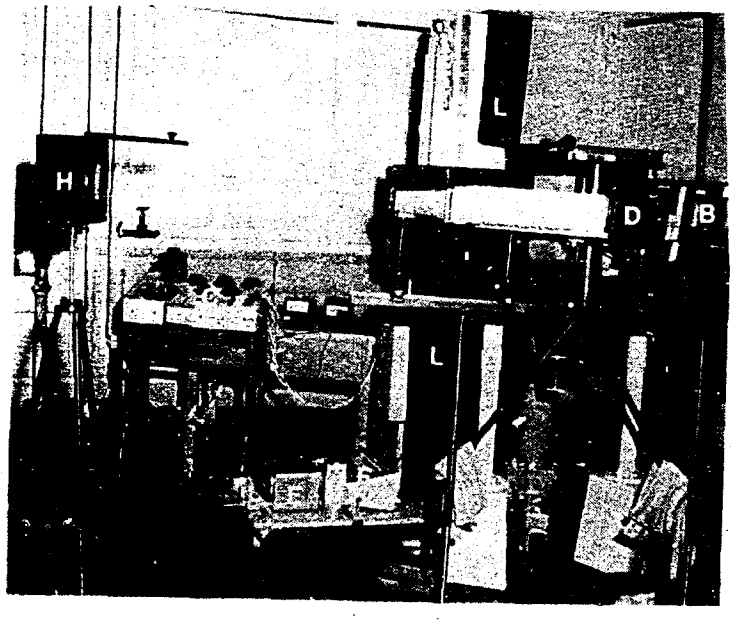

Figure 1

Test Apparatus

A	Test Model	G	Ice Bath
B	Interferometer	H	Parabolic Mirror
C	Plate Temperature Control Panel	I	Interferometer Leveling Jacks
D	Camera	J	Voltmeter
E	Potentiometer	K	Ammeter
F	Thermocouple Switch Board	L	Air Current Baffles

Heated Vertical Plate

The heated vertical plate was constructed of aluminum and measured 8 in wide by 50 in long. It was mounted on an adjustable stand which allowed for vertical adjustment of the entire plate. The test plate was constructed with a 26 in long leading edge and four identical aluminum blocks (2 in thick by 6 in high by 8 in wide). One of the four blocks had a rectangular cavity milled across the width of the block. The cavity width b was held constant at 1 in while the depth d was varied in increments of 0.2 in (0.2 in to 0.6 in). The leading edge and each of the four blocks had separate nichrome wire heaters. This allowed for a plate temperature variance of not more than ± 1.0 R over the entire length. The test stand provided for rotation about three orthonormal axes. This rotation was necessary to properly

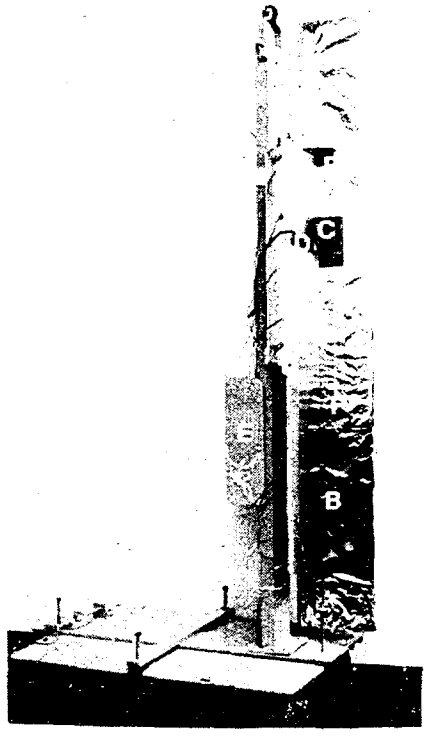

Figure 2

Test Stand with One Side Shield Removed

A Heated Vertical Plate
B Side Shield
C Window
D Rectangular Cavity
E Counterweights
F Plexiglass Scale
G Alignment Apparatus

align the cavity with the light beam. Figure 2 shows the plate with one side shield removed.

Interferometer

The interferometer which was used was a Mach-Zehnder type with 6 in diameter optical parts. The light source was provided by a mercury lamp which together with a Wratten 77A filter yielded a green light with a wavelength of 5461 angstroms.

Camera

A 3 by 5 in Garflex camera with a frosted glass screen, conventional film holder, and Polaroid back was used throughout the study. All pictures were taken on Polaroid type 47 film, ASA 3000. A shutter speed of 1/400 second was used throughout the study.

Potentiometer

A Honeywell potentiometer was used to measure the potential across the iron-constantan thermocouples. The potentiometer was graduated in 0.02 millivolt intervals (representing about 0.6 R) and an ice water bath was used as the reference.

Temperature Control Panel

The power to the heaters was controlled by means of one Variac and five Powerstat voltage regulators. The Variac voltage regulator was used to control the temperature of the leading edge section. Four Powerstats were used to control the temperature of the four test blocks. The fifth Powerstat was connected in series with each of the other Powerstats and it was used to control the overall temperature of the test blocks.

III. Experimental Procedures

Two series of tests were run during this study: the flat plate series and the cavity series. Consequently, two slightly different sets of procedures were used. The plate to ambient temperature difference was held constant at 130 R (±1 R) for both series of tests. The following is a summary of the procedures. The reader is referred to Appendix C for a more detailed presentation.

Flat Plate Procedure

Interferograms, necessary to calculate the heat transfer rate, were obtained for all stations from 26.2 to 49.0 in from the leading edge.

The first step in obtaining interferograms was to position the test plate (up or down) so that the section to be studied would be located in the interferometer test section. The plate was then adjusted so that it was vertical as indicated by a carpenter's level. The final step, prior to turning the heaters on, was to align the plate (Appendix C) such that the light rays were parallel to the face of the plate. The plate heaters were then turned on. After the desired temperature difference and equilibrium were obtained (2-4 hours), the interferometer was then adjusted using the "infinite fringe" method of adjustment. The interferograms were then taken on Polaroid film.

Cavity Study Procedure

One of the blocks which makes up the plate surface was milled to form a rectangular cavity along the width of the block. The cavity

width was 1 in and the depth was 0.2 in. After the series of tests with this depth were completed, the cavity depth was increased to 0.4 in, and then finally to 0.6 in. By interchanging blocks each cavity was located at four elevations: 26.7, 32.7, 38.7, and 44.7 in from the leading edge.

The block with the cavity was placed in the desired position in the test plate and then the entire plate was positioned in the same manner as the flat plate. The alignment procedure (Appendix C) for this series of tests was complicated by the fact that the horizontal cavity walls (expansion and recompression) also had to be parallel with the interferometer light rays. After the desired temperature difference had stabilized, it was found that further "fine" adjustments could be made by observing the fringe closest to the plate. The plate was aligned when the first fringe could be seen throughout the cavity. The interferograms were then obtained on Polaroid film.

IV. Data Analysis

In free convection from a vertical flat plate, the heat transfer rate is given by Newton's equation.

$$q = h(T_p - T_a) \tag{1}$$

or

$$q = h\theta \tag{2}$$

The conduction equation applied at the plate surface yields

$$q = -k \left(\frac{\partial T}{\partial y}\right)_p \tag{3}$$

Equating eq 2 to eq 3 yields

$$h = -\frac{k}{\theta} \left(\frac{\partial T}{\partial y}\right)_p \tag{4}$$

An average temperature gradient at the plate surface was determined by analyzing four interferograms (see Fig 3 for sample interferogram) and averaging the results. Fringe location measurements were made at 1/2 in intervals over a distance of approximately 4 in on each interferogram in the smooth flat plate test.

The "infinite fringe" method of adjustment was used throughout the study, but at the higher elevations the boundary layer extended beyond the field of vision of the interferometer light beam which made it difficult to determine when this adjustment existed. The interferometer was considered to be properly adjusted when the distance between the fringes at the outermost edge of the thermal boundary layer was a maximum. Both methods yielded the same results; this was

determined by comparing the results of interferograms taken by the two methods. The fact that all the fringes could not be observed due to the narrow field of vision of the interferometer yielded another problem. Namely, there was no area in the interferograms which could be used as a reference area, i.e., all physical properties are known. It was assumed that the light area immediately adjacent to the plate surface was at plate temperature and room pressure thereby providing a reference area. This was adequate since it was the temperature gradient and not the absolute temperature represented by the fringes that was of interest, the error that this assumption caused was shown to be negligible.

Figure 3

Sample Interferogram

The density in the reference area was calculated from the ideal gas equation and the densities represented by each of the first three fringes were determined from the interferometer equation

$$\rho_n = \rho_p + \left(\frac{\rho_0 \lambda_0}{\eta_0 - 1}\right)\left(\frac{1}{W}\right)(n-0.5) \qquad (5)$$

where n was the fringe number (1,2,3) and

$$\frac{\rho_0 \lambda_0}{\eta_0 - 1} = 5.1 \times 10^{-4}\ lb_m/ft^2 \qquad (6)$$

The ideal gas equation was then used to determine the temperature at each of the first three fringes. A micro-comparator was then used to obtain the spacings between these fringes. The temperature difference between each of the first two pairs of fringes was then averaged and divided by the corresponding spacing to obtain the temperature gradient at the plate surface. This was the method used by both Shine (Ref 13:60) and Fletcher (Ref 7:8).

The heat transfer rate was determined at 0.5 in intervals at elevations from 26.5 in to 49.0 in for the flat plate. When the cavity tests were run, heat transfer rates were determined by this method below and above the cavity (Fig 4).

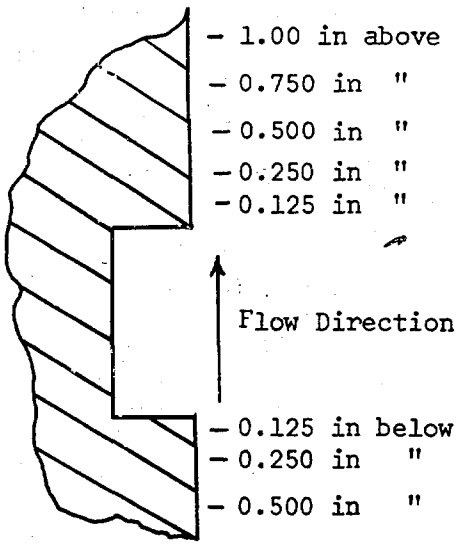

Figure 4

Locations of Readings About Cavity

The data reduction calculation was accomplished using the AFIT IBM 1620 computer. Appendix D contains the explanation of the computer programs used.

Internal Cavity Analysis

The heat transfer rate from each of the three walls was calculated from eq 3 where the value of the thermal conductivity of air at 200 F was used. The temperature gradient was taken to be the difference between the known wall temperature and the determined temperature represented by the first fringe divided by the distance from the wall to the first fringe. The total heat transfer from the three walls by conduction was assumed to be equal to the heat transferred by convection across an imaginary surface covering the cavity opening.

V. Results and Discussion

The interferograms that showed the lower portion of the plate gave visual evidence of the transition from laminar to turbulent flow at elevations between 29 in and 33 in (see Fig A-2). This corresponds to Grashof numbers of 2.56×10^9 and 4.0×10^9 which compares favorably to the results of both Bayley and Cheeswright. Quantitatively, this transition is shown in the variation of the heat transfer coefficient with plate height as may be seen in Fig 5.

Equation 7 describes the relationship between Nu and Gr at the lower portion of the plate (26 in to 30 in). It should be noted that the Nusselt and Grashof numbers in eq 7 are the average values computed over the 4 in area. The coefficient in eq 7 is also an average value. The computed values of the coefficient varied from 0.365 at an elevation of 26.5 to 0.325 at 30.0 in elevation.

$$\overline{Nu} = 0.340(\overline{Gr})^{0.25} \tag{7}$$

This relationship compares favorably with the results (eq 8) of Schmidt and Beckmann (Ref 12:45) and Fletcher (Ref 7) for laminar free convection. This indicates that the flow was laminar between the elevations of 26 in to 30 in.

$$\overline{Nu} = 0.360(\overline{Gr})^{0.25} \tag{8}$$

At the upper portion of the plate the following relationship was found to best describe the heat transfer rate.

$$\overline{Nu} = 0.11(\overline{Gr}\ \overline{Pr})^{1/3} \tag{9}$$

The Prandtl number in the above equation was obtained from the gas tables.

This result can be compared to the results of McAdams (Ref 11) for the heat transfer rate to a turbulent boundary layer (eq 10).

$$\overline{Nu} = 0.13(\overline{Gr}\ \overline{Pr})^{1/3} \tag{10}$$

Figures 7, 8, 9 and 10 show the effect of cavity depth on the heat transfer rate, from various areas of the plate, as compared to the heat transfer rate of the smooth flat plate. It is evident that the lowest heat transfer rate occurred at the expansion wall and the concave corner formed by this wall and the bottom wall. The highest heat transfer rate occurred at the recompression wall. This is due to the fact that this wall contains a stagnation point and the temperature gradient is largest at this point due to the outer (cooler) boundary layer flowing into the cavity and against the recompression wall.

The heat transfer rate from the bottom of the cavity decreased as the cavity depth was increased, but this dependence diminished as the turbulence level (Gr) increased. This decreased dependence is the result of the dominating mechanism of heat transfer switching from the viscous shear (microscopic) to the random motion of eddies of air (macroscopic) as the Grashof number increases.

The areas, 0.5 in below and 1.0 in above the cavity, experienced an increase in the heat transfer rates compared to those of the smooth flat plate. This increase did not appear to be a function of the cavity depth, but merely of the presence of the cavity. The cavity introduced an additional perturbation in the boundary layer near the

two corners (which increased the turbulence in the flow). This had a greater effect on the heat transfer rate downstream of the cavity than upstream.

Figure 11 portrays the overall or net effect of the cavity on the convection coefficient compared to the coefficient for the smooth flat plate. The ratio of the coefficients with the cavity to that without the cavity, h/h_f, was evaluated for the 2.5 in plate height over which the cavity had an effect. The cavity increased the net heat transfer rate substantially (up to 41%) from the lower portion of the plate ($2.0\times10^9 < Gr < 4.0\times10^9$), but the increase tapered down to no effect at a height of about 40 in. This increase was attributed to the fact that the boundary layer was laminar at the lower elevations for the smooth flat plate but the boundary layer was turbulent (at least in the outer portion) when the cavity was introduced. Figure 5 illustrates this behavior. It should be noted that the points plotted for the cavity study are independent and that they are the average values over the elevations as indicated. As the fully developed turbulent flow field was formed at the higher plate positions, the effect of the cavity was to decrease the heat transfer rate (maximum decrease was 25%). This decrease is attributed to the development of hot vortices in the cavity which act as pseudo-heat sources much like those observed by Fox (Ref 8) and Chapman (Ref 2) in their forced convection studies.

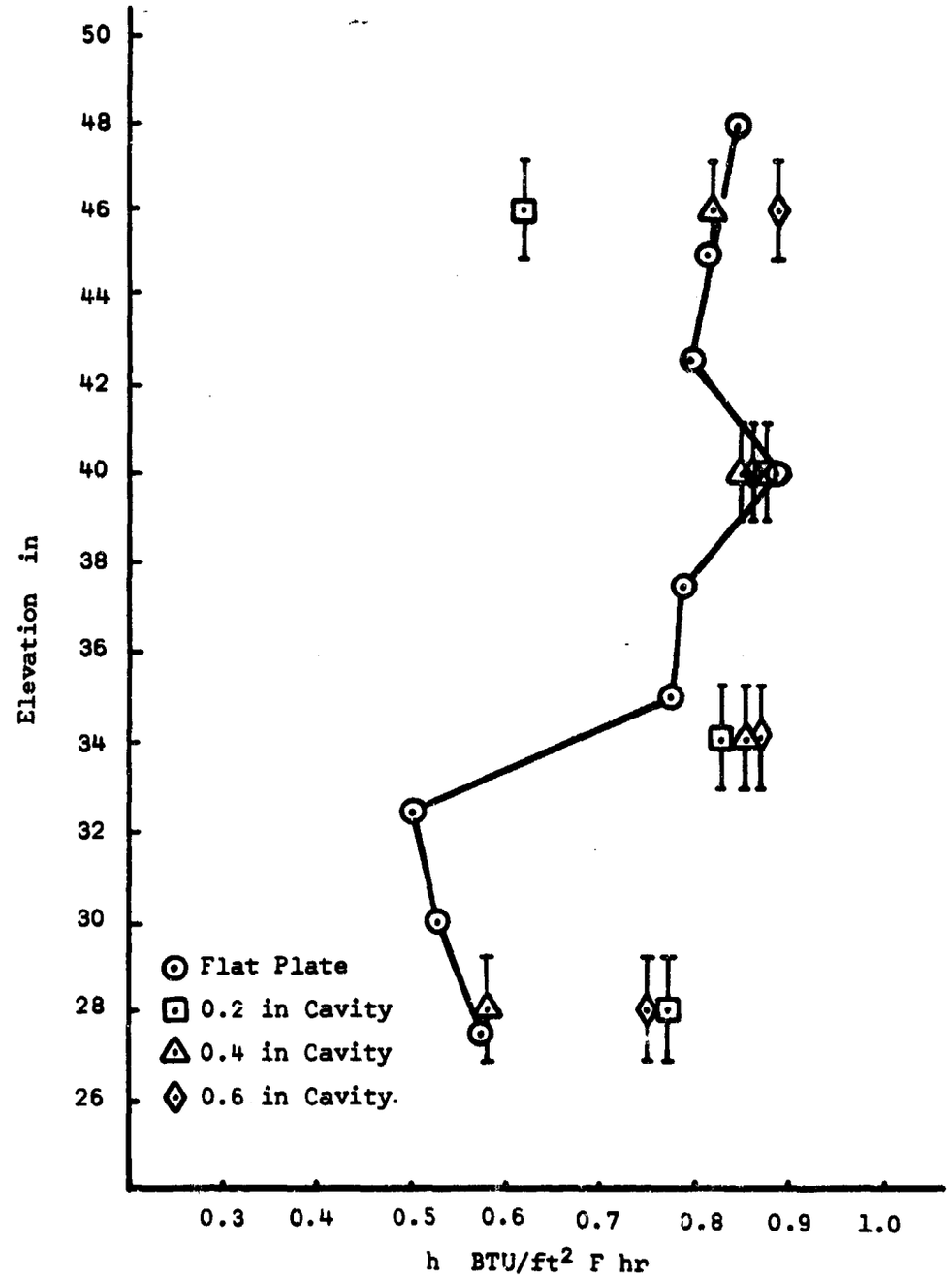

Figure 5

Effect of Cavity Depth on the Convection Coefficient of Heat Transfer

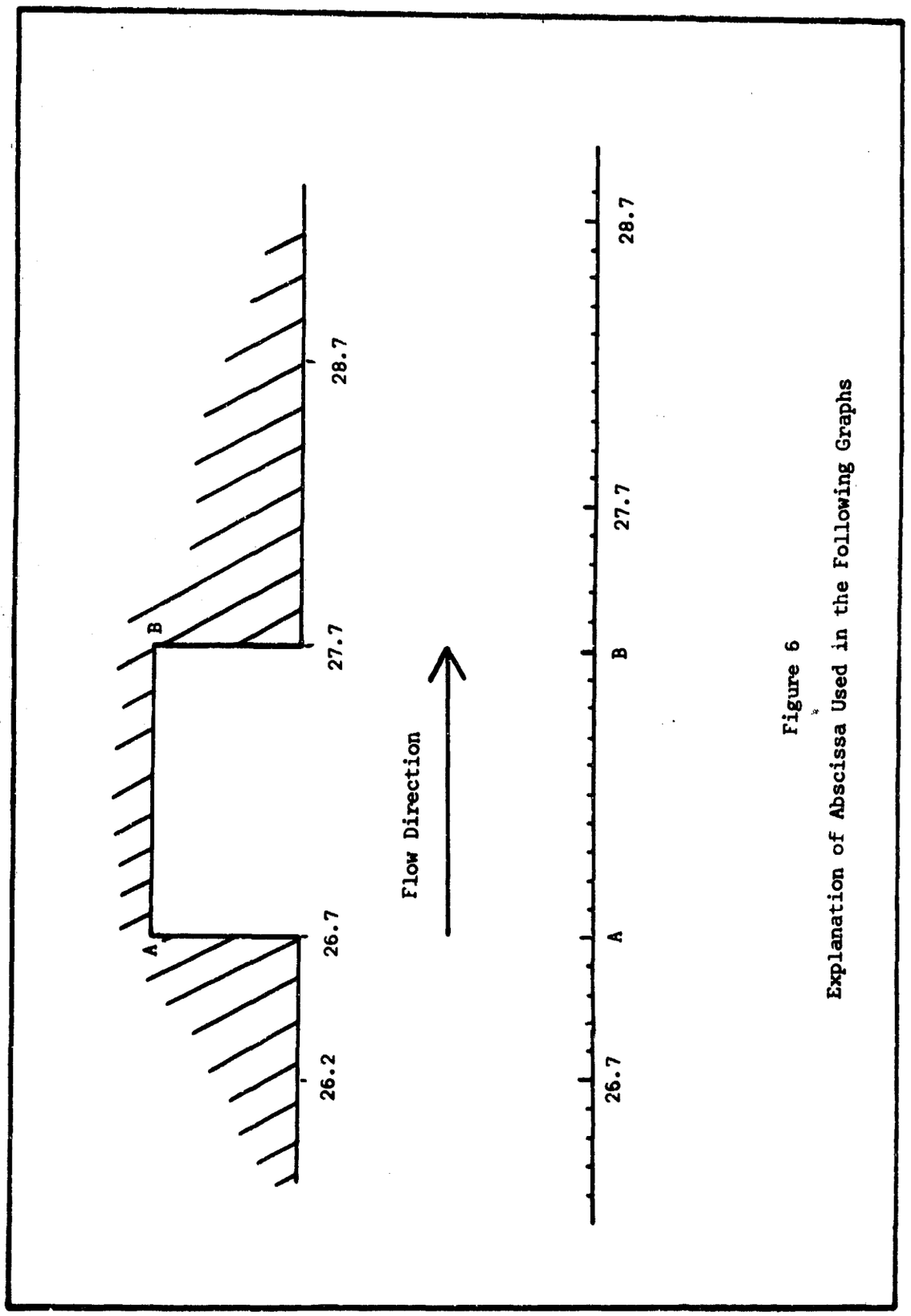

Figure 6

Explanation of Abscissa Used in the Following Graphs

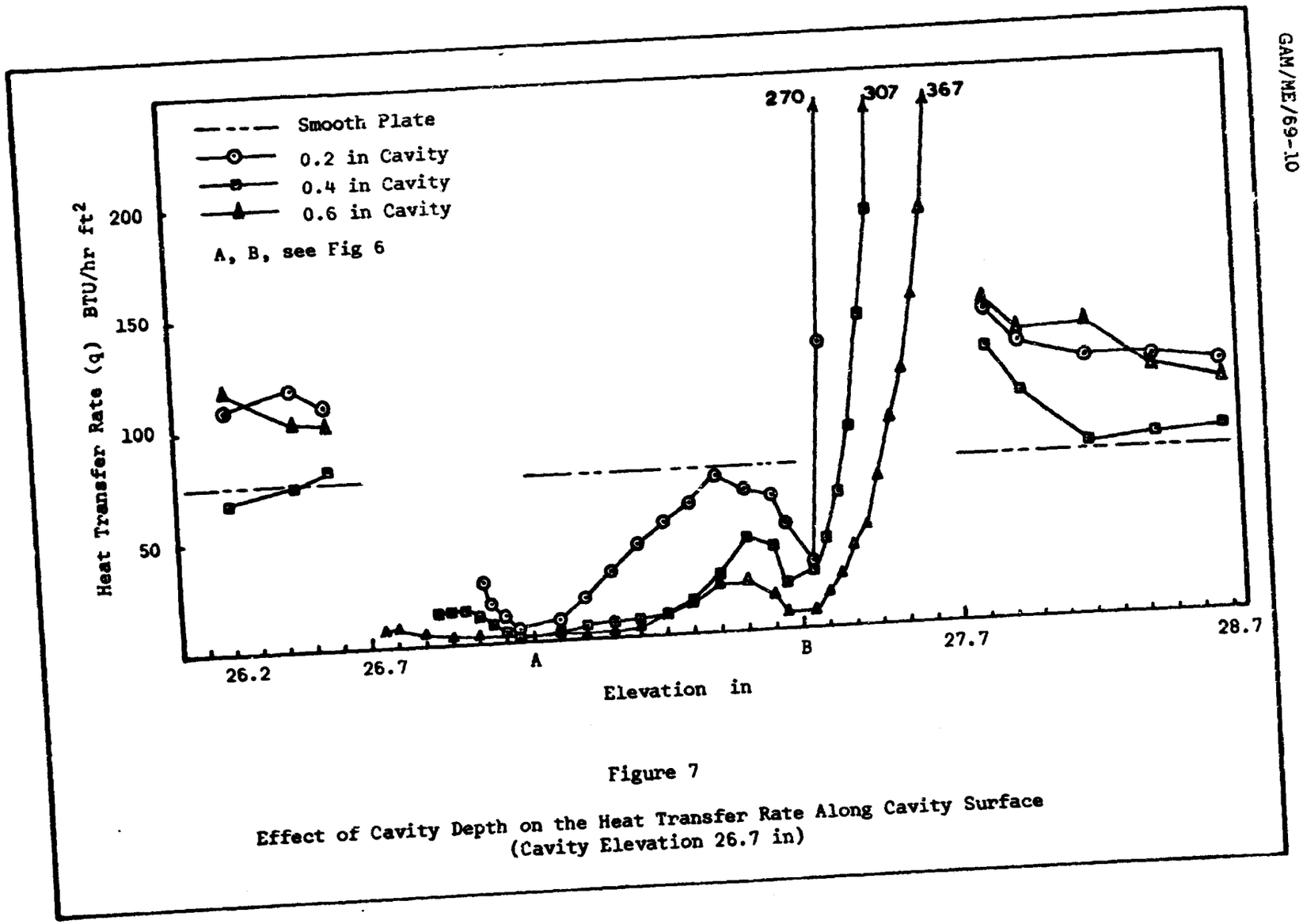

Figure 7

Effect of Cavity Depth on the Heat Transfer Rate Along Cavity Surface
(Cavity Elevation 26.7 in)

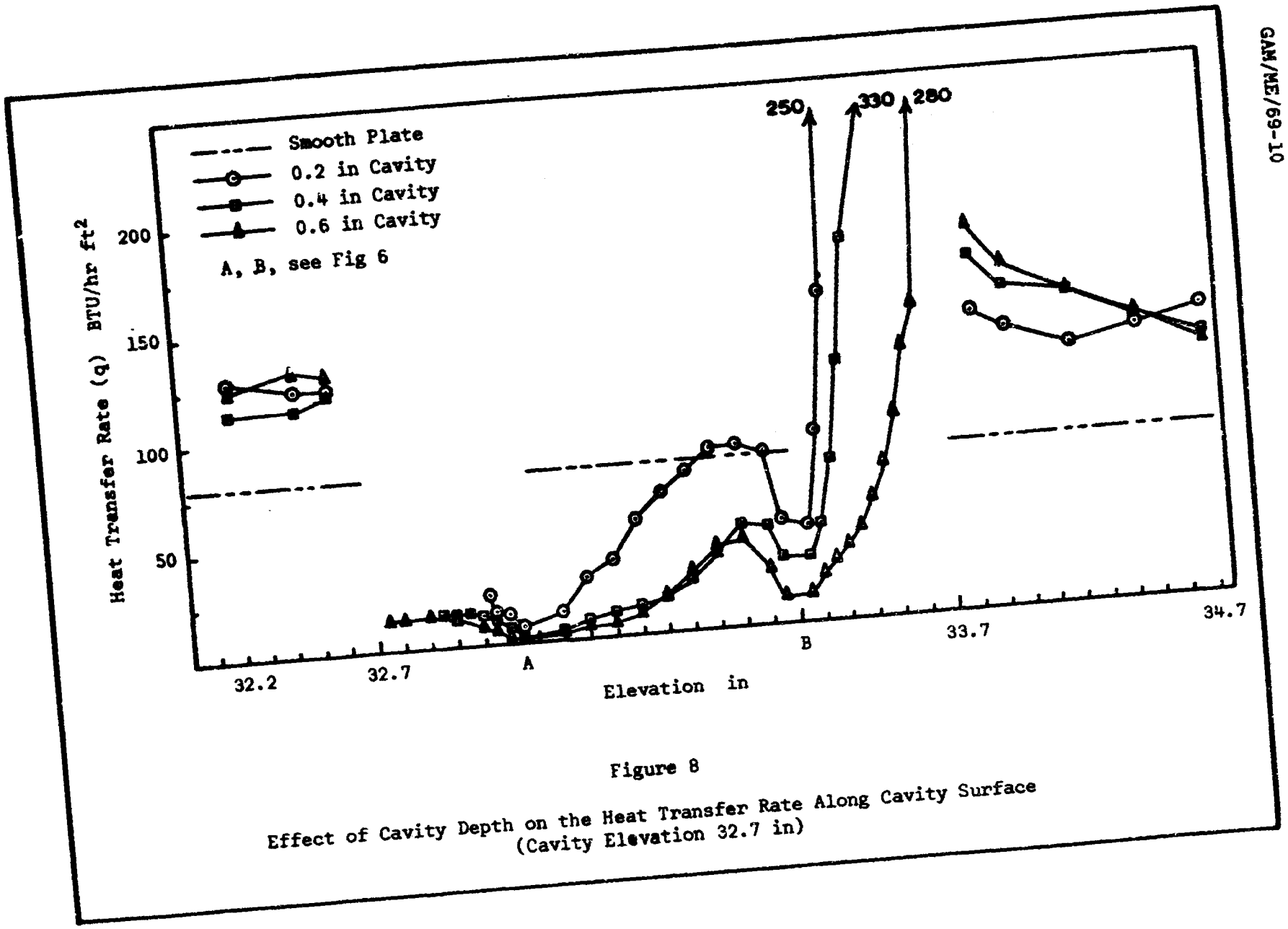

Figure 8

Effect of Cavity Depth on the Heat Transfer Rate Along Cavity Surface
(Cavity Elevation 32.7 in)

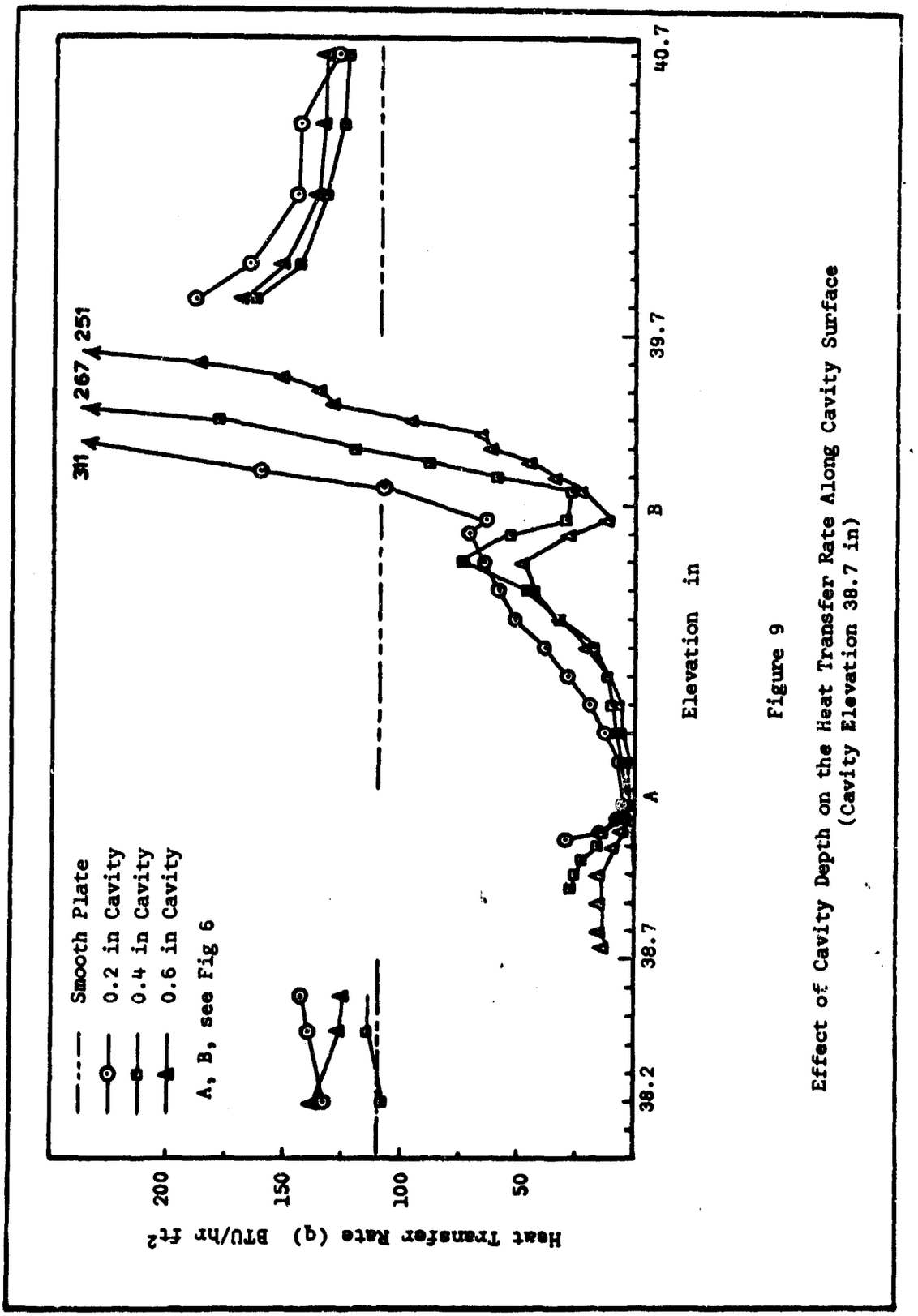

Figure 9

Effect of Cavity Depth on the Heat Transfer Rate Along Cavity Surface
(Cavity Elevation 38.7 in)

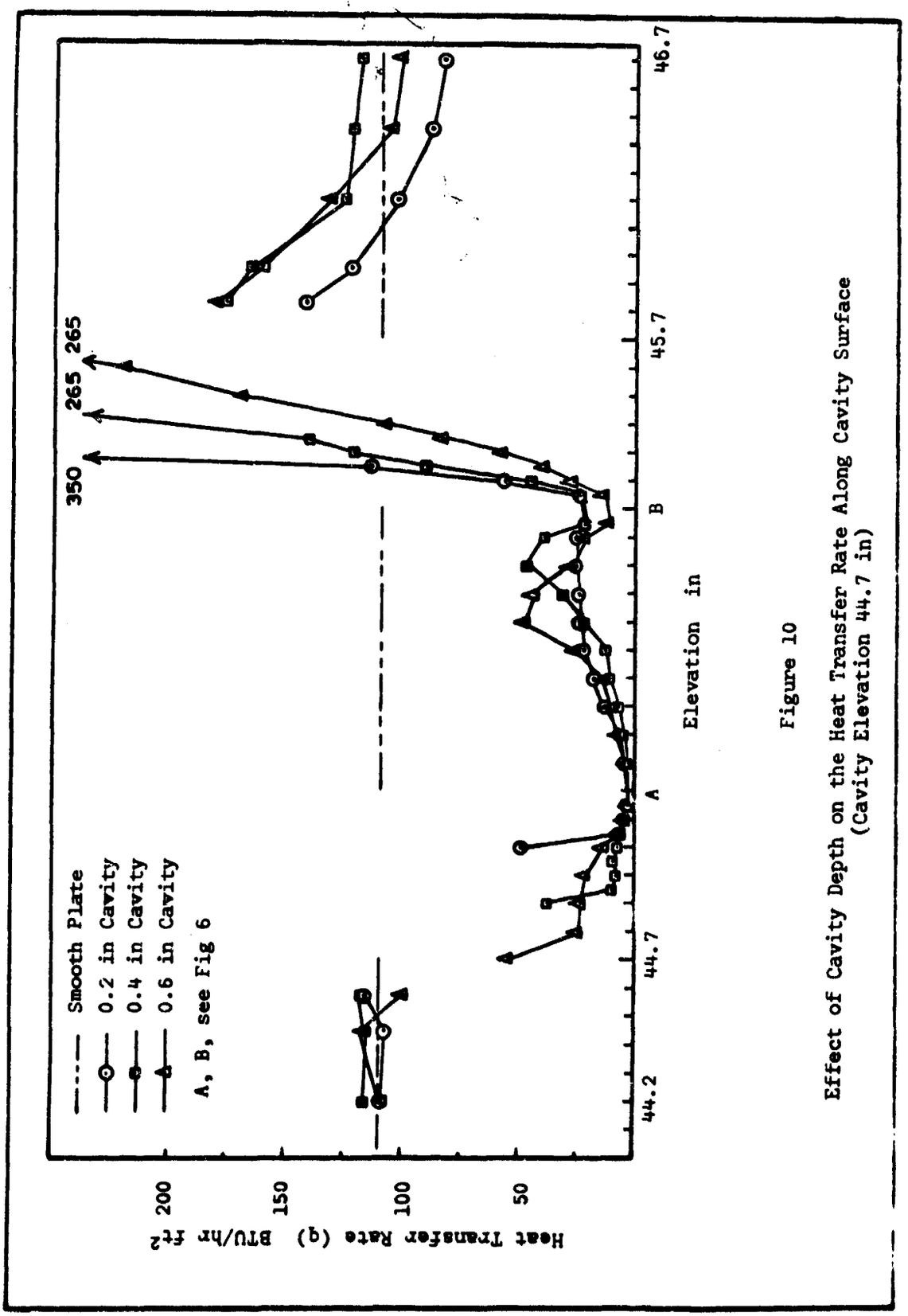

Figure 10

Effect of Cavity Depth on the Heat Transfer Rate Along Cavity Surface
(Cavity Elevation 44.7 in)

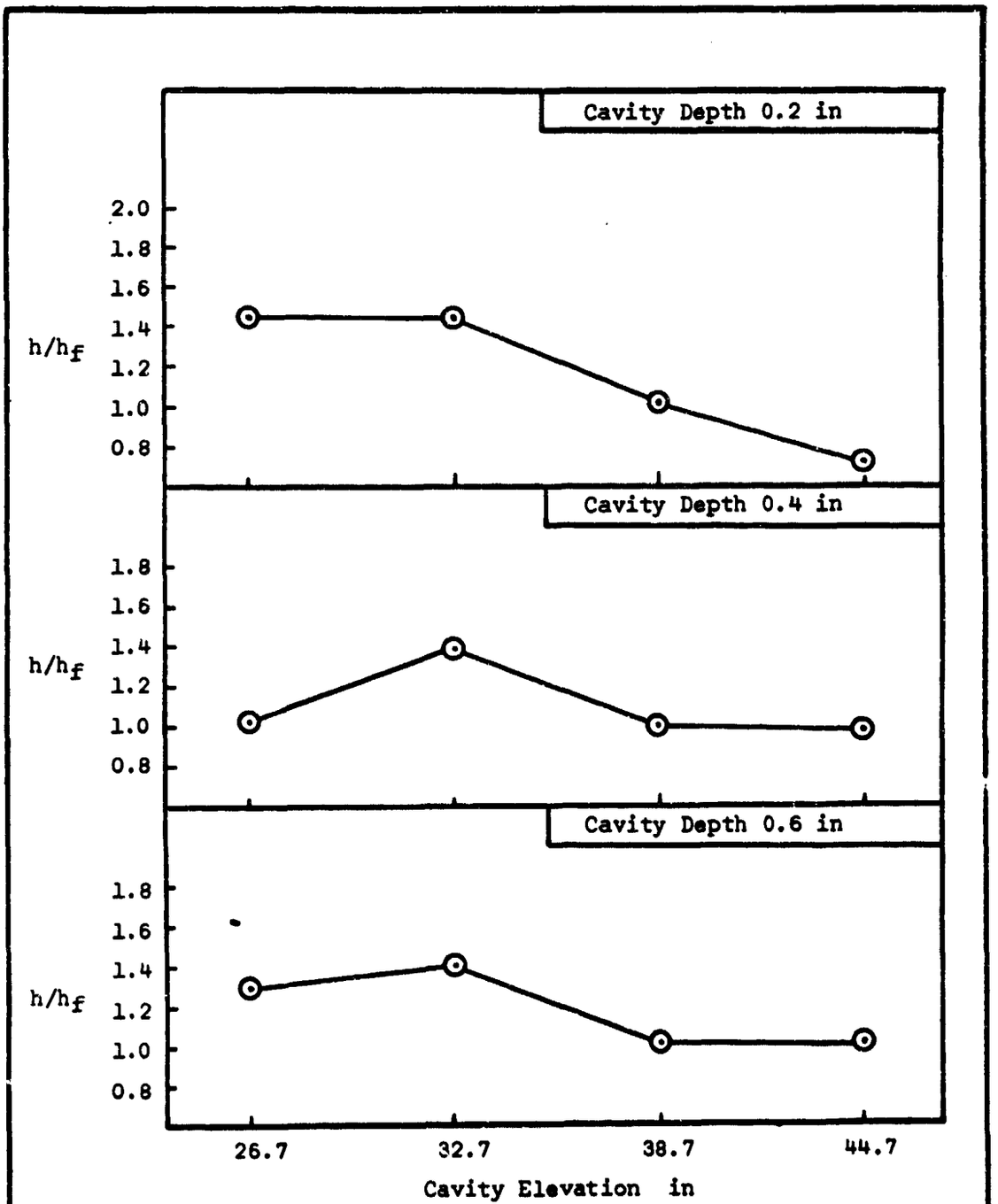

Figure 11

Overall Effect of Cavity on the Convection Coefficient of Heat Transfer over the 2.5 in Distance Affected by the Cavity

VI. Conclusions

Based on the results of this study, the following conclusions were drawn:

1. The effect of the cavity on the net heat transfer rate was dependent on the type of flow (Grashof number). The cavity caused an increase in the net heat transfer rate when the flow was laminar or transitional ($2.5\times10^9 < Gr < 10^{10}$) and it caused a decrease in the heat transfer rate in the turbulent flow region ($Gr < 10^{10}$) for cavity depths of 0.4 and 0.2 in. The maximum increase of 41% was obtained at a cavity elevation of 26.7 in and the maximum decrease of 25% was obtained at a cavity elevation of 44.7 in. The increase of 41% was approximately 5 times the increase that Fletcher had observed in his laminar study. These effects were observed over a 2.5 in distance along the plate in the vicinity of the cavity.
2. The area of maximum heat transfer rate occurred at the recompression wall and was the dominating factor in determining the net effect on the overall heat transfer rates due to the cavity.
3. The effect of the cavity depth on the net heat transfer rate was inconsequential at all elevations, but the cavity depth had a marked effect on the heat transfer rate from the bottom surface of the cavity in the lower portion of the plate where the rate decreased as the cavity depth was increased.
4. The transition point from laminar to turbulent flow began at $2.5\times10^9 < Gr < 4.0\times10^9$.

VII. Recommendations

The following recommendations are made:

1. To better understand the mechanism of heat transfer over irregular surfaces, cavities of various other shapes should be studied. A wedge shaped cavity is suggested. Because of the low heat transfer rate from the expansion wall found in this study, it is expected that the wedge results would be similar to the rectangular cavity results. It is suggested that if the apparatus of this study is to be used again, it should be modified by replacing two 6 in long blocks with a single block 12 in long. Mill an oversized cavity (approximately 2 in wide by 1.75 in deep) across the face of the block to accept inserts, with the various geometric cavities machined in these inserts. This method would have several advantages over the method used in this study. It would be possible to make reruns without reconstructing an entire new test block; it would eliminate wasted time waiting for machining to be accomplished; and it would greatly increase the versatility of the apparatus.
2. The study be continued with an increased temperature difference (approximately 230 R). This would increase Gr to 1.1×10^{11} and thereby ensure a turbulent flow field.
3. A hot wire or hot film anemometer be employed to check the temperature and velocity flow fields. This instrument is particularly well suited for a turbulent flow study (Ref 9:202).

Bibliography

1. Bayley, F.J. "An Analysis of Turbulent Free Convection Heat Transfer." Proc. Institution of Mechanical Engineers, 169(20), 361-370 (1955).

2. Chapman, D.R. A Theoretical Analysis of Heat Transfer in Regions of Separated Flow. NACA TN 3792, (1956).

3. Cheeswright, R. "Turbulent Natural Convection From a Vertical Plane Surface." Journal of Heat Transfer, 1-8 (February 1968).

4. Dhanak, A.M. and Haugen, R. "Heat Transfer in Turbulent Boundary - Layer Separation Over a Cavity Surface." Journal of Heat Transfer, 340-355 (November 1967).

5. Eckert, E.R.G. and Soehnghen, E. "Interferometer Studies on the Stability and Transition to Turbulence of a Free Convection Boundary Layer." Proceedings of the General Discussion on Heat Transfer, ASME, 321-323 (1951).

6. Emery, A.F., et al. "Heat Transfer and Pressure Distribution in Open Cavity Flow." Transactions of the ASME, 106-108 (February 1967).

7. Fletcher, C.C. The Effect of a Transverse Notch on the Heat Transfer Rate From a Heated Vertical Plate in Free Convection. Thesis. Air Force Institute of Technology (AU), Wright-Patterson Air Force Base, Ohio, 1966.

8. Fox, J. "Heat Transfer and Air Flow in a Transverse Rectangular Notch." International Journal of Heat Mass Transfer, 8:269-279 (1965).

9. Holman, J.P. Experimental Methods for Engineers (1st). New York: McGraw-Hill, 1966.

10. Kreith, F. Principles of Heat Transfer (2nd). Scranton, Pennsylvania. International Text Book Company, 1966.

11. McAdams, W.H. Heat Transmission (3rd). New York: McGraw-Hill, 1954.

12. Schmidt, E. and Beckmann. "Das Temperatur- und Geschwindigkeitsfeld vor einer Waerme abgebenden senkrechten Platte bei natuerlicher Konvektion." Techn. Mechanik u. Thermodynamik, (1), 341-64 (1930).

13. Shine, A.J. The Effect of Transverse Vibrations of the Heat Transfer Rate From a Heated Vertical Plate in Free Convection. PhD Dissertation. Columbus, Ohio: The Ohio State University, 1957.

Appendix A

Sample Interferograms

Three representative sets of interferograms are presented.

Figure A-1 shows the effect of cavity depth on the interferogram patterns at a single elevation (44.7 in). This set of interferograms shows the formation of the vortex in the 0.6 in cavity. This set also shows that as the cavity depth is increased, the temperature gradient at the expansion wall is increased.

From Fig A-2 the effect of elevation change on the interferogram patterns (cavity depth 0.4 in) may be viewed. The increase in turbulence is well exhibited in this set of photographs.

Figure A-3 shows the variation of the interferogram patterns with time for a cavity depth of 0.6 in and an elevation of 44.7. It can be seen that the heat transfer rate calculated from any two of these interferograms would not be the same. This is why four interferograms at each location and cavity depth were analyzed.

Smooth Flat Plate

0.2 in Deep Cavity

0.4 in Deep Cavity

0.6 in Deep Cavity

Figure A-1

Interferograms Showing the Effect of Cavity Depth (Cavity Elevation 44.7 in)

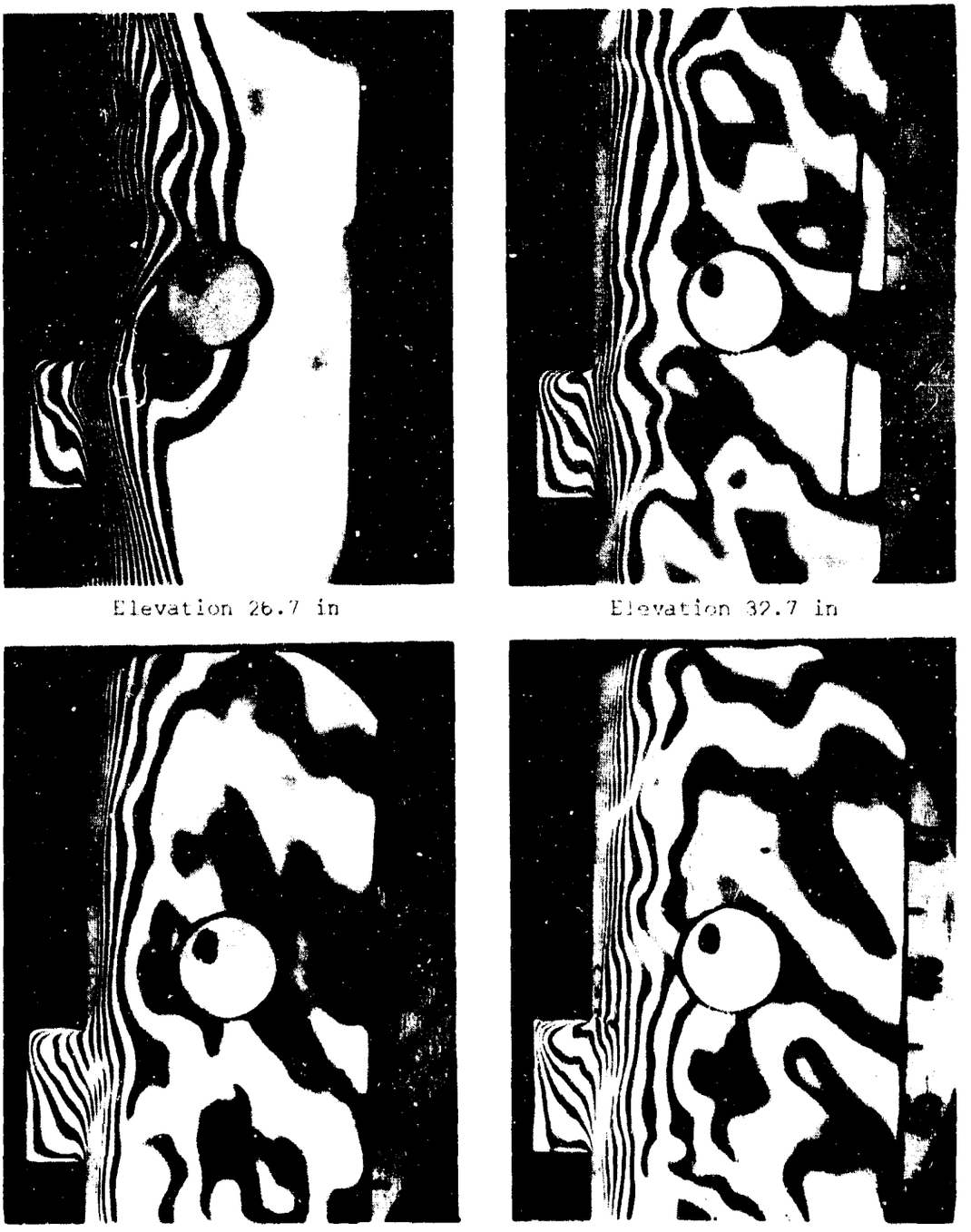

Elevation 26.7 in

Elevation 32.7 in

Elevation 38.7 in

Elevation 44.7 in

Figure A-2

Interferograms Showing the Effect of Elevation
(Cavity Depth 0.4 in)

Figure A-3

Variation in the Interferograms with Time (Cavity Depth 0.6 in, Elevation 32.7 in)

Appendix B

Apparatus

The apparatus used for this study was basically the same as that of Fletcher. The major difference was the addition of a 26 in long leading edge assembly (Fig B-1). This leading edge assembly consisted of four parts: the aluminum leading edge plate (Fig B-2), the nichrome heating grid, the asbestos insulation and the plywood backboard. The aluminum leading edge plate was designed to fit the existing apparatus. The nichrome heating grid and the asbestos insulation was sandwiched between the aluminum plate and the plywood backboard. This design provided for quick and efficient temperature control of the leading edge plate. Other modifications included the construction of longer side shields and air baffles which were added to minimize outside disturbances.

The entire test stand was placed on a wood dolly which together with the alignment device (Fig B-8) greatly decreased alignment times.

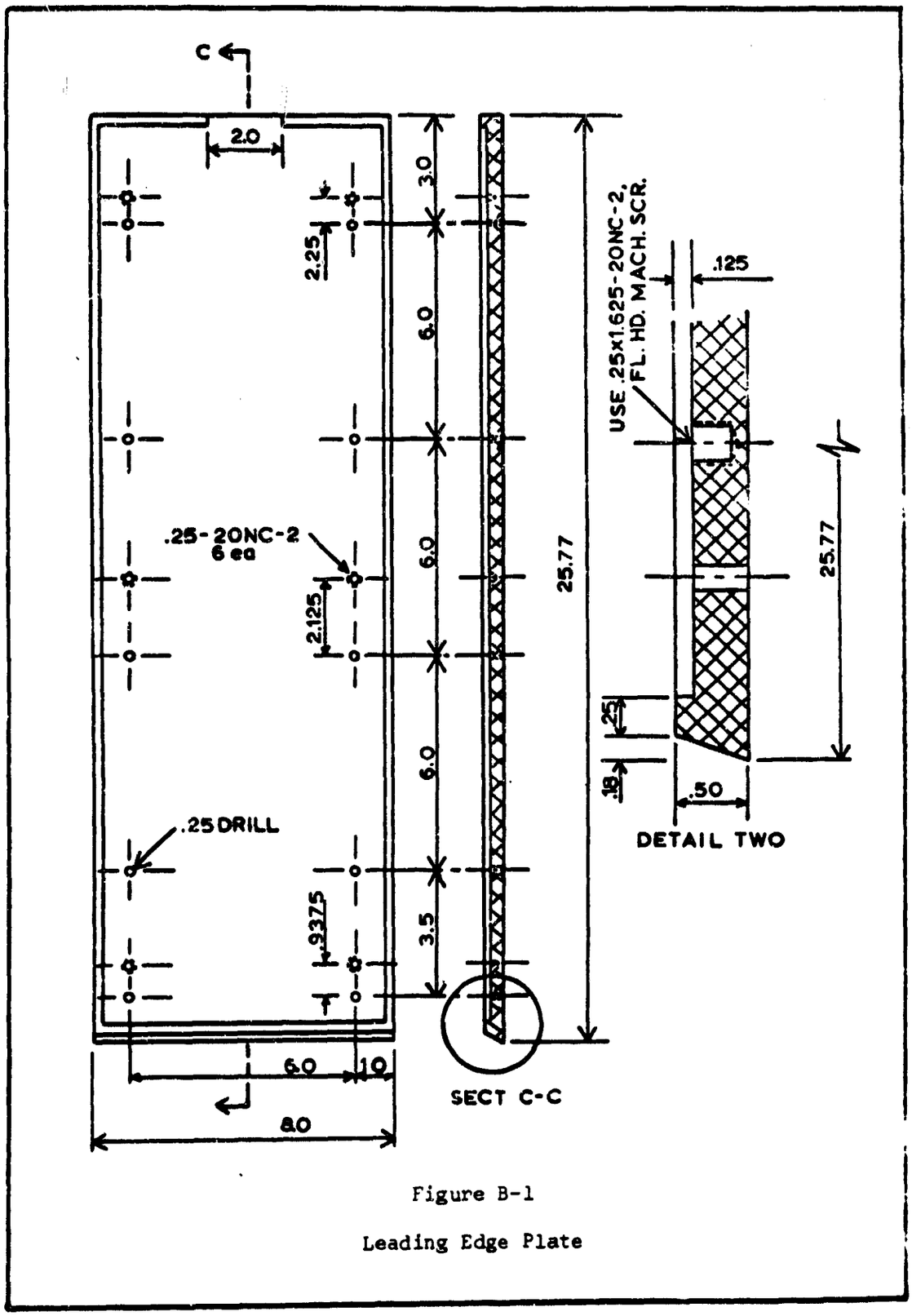

Figure B-1

Leading Edge Plate

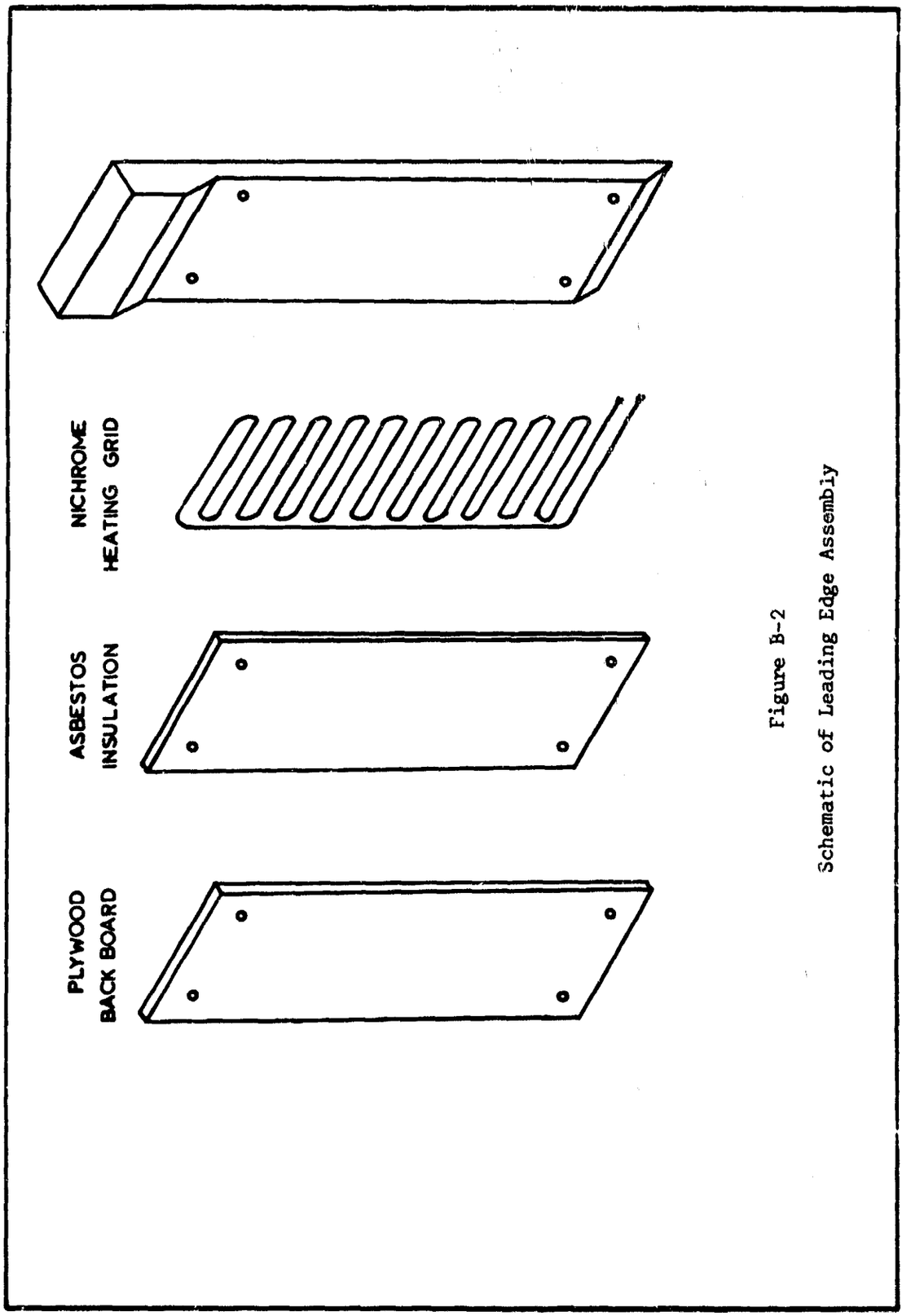

Figure B-2

Schematic of Leading Edge Assembly

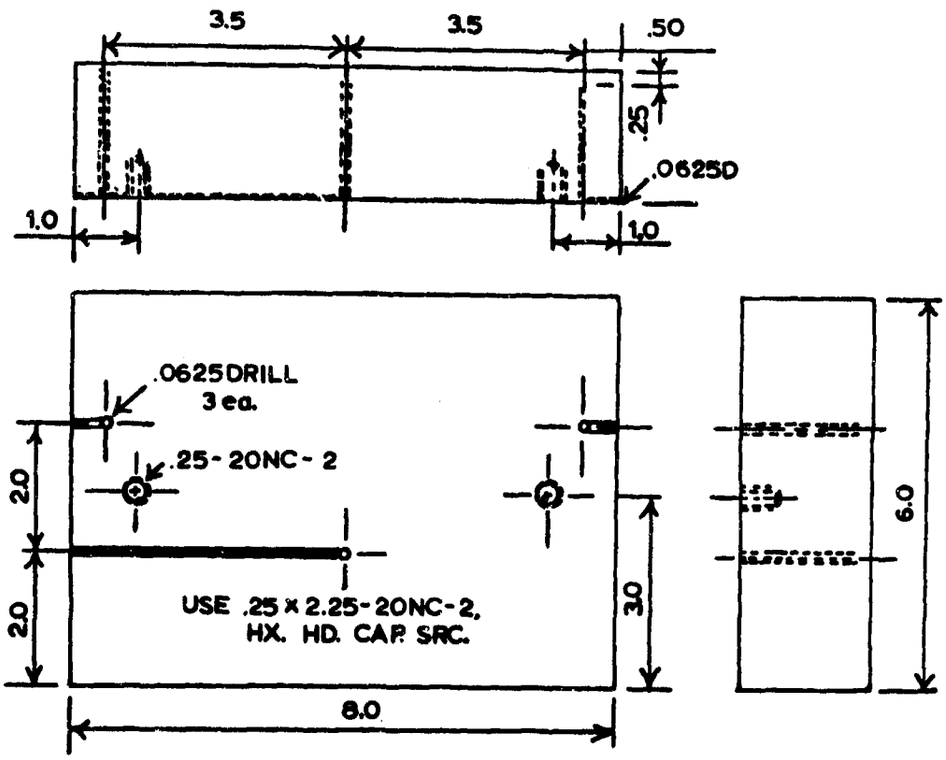

Figure B-3

Plate Segment

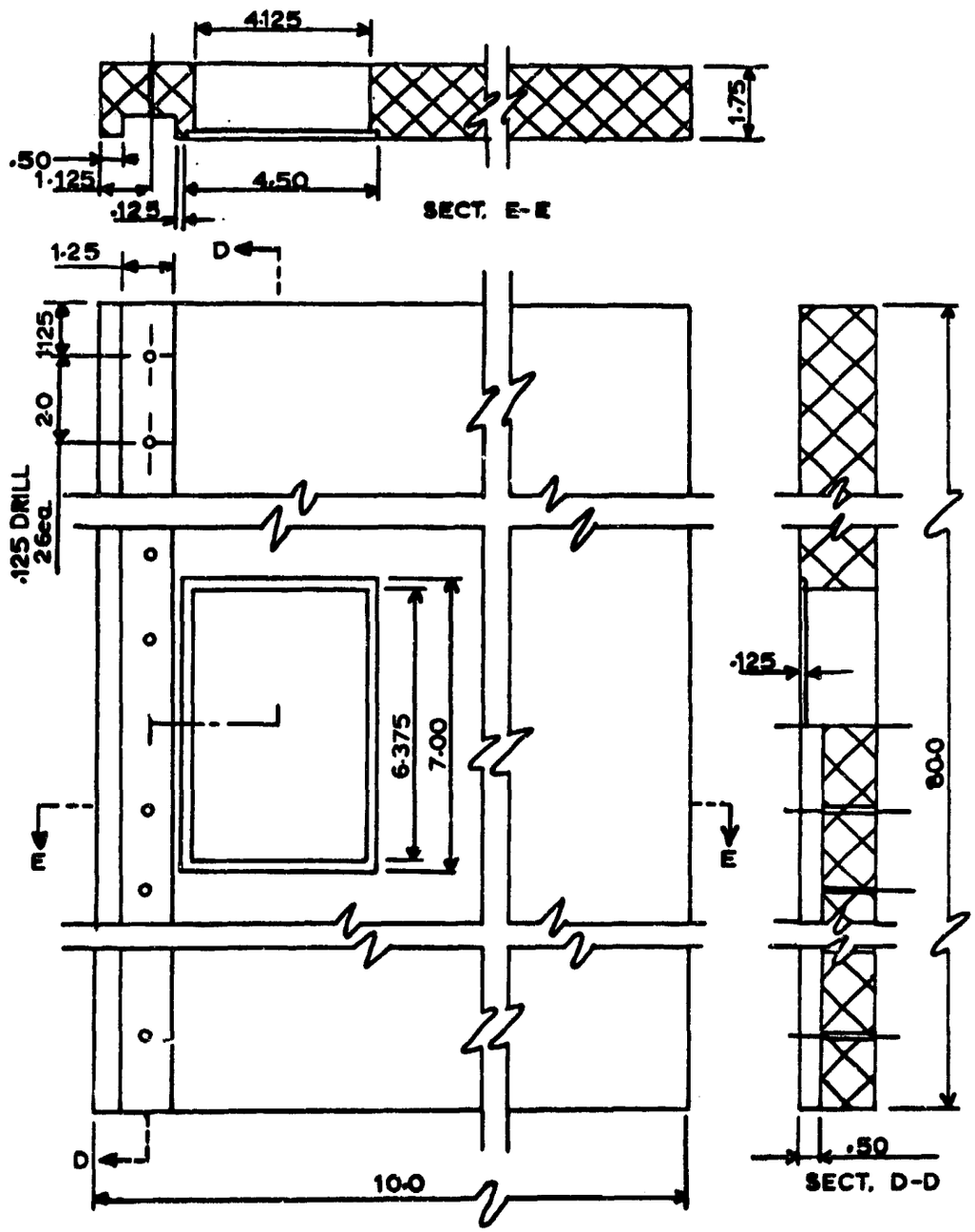

Figure B-4

Side Shield

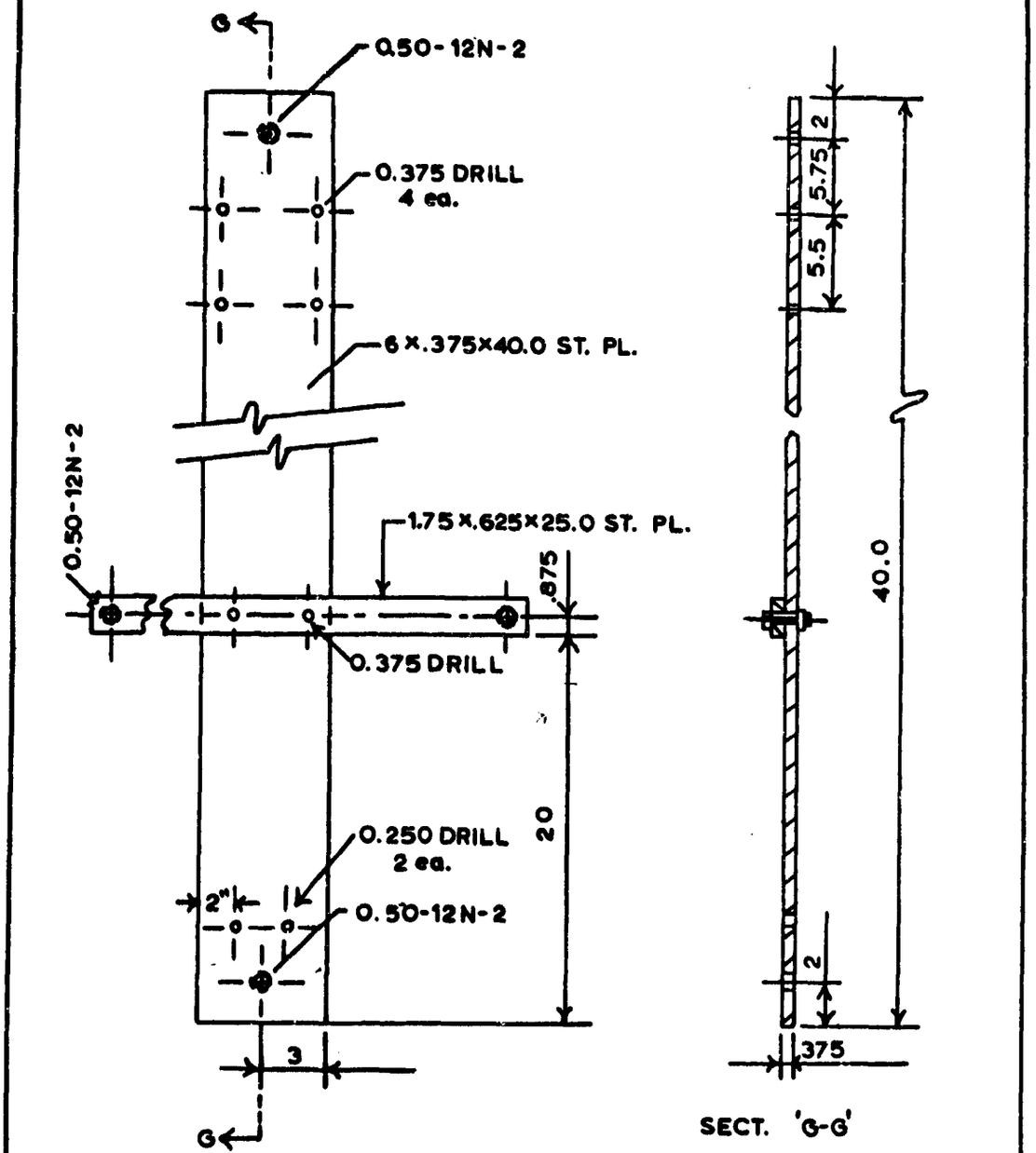

Figure B-5

Support Stand

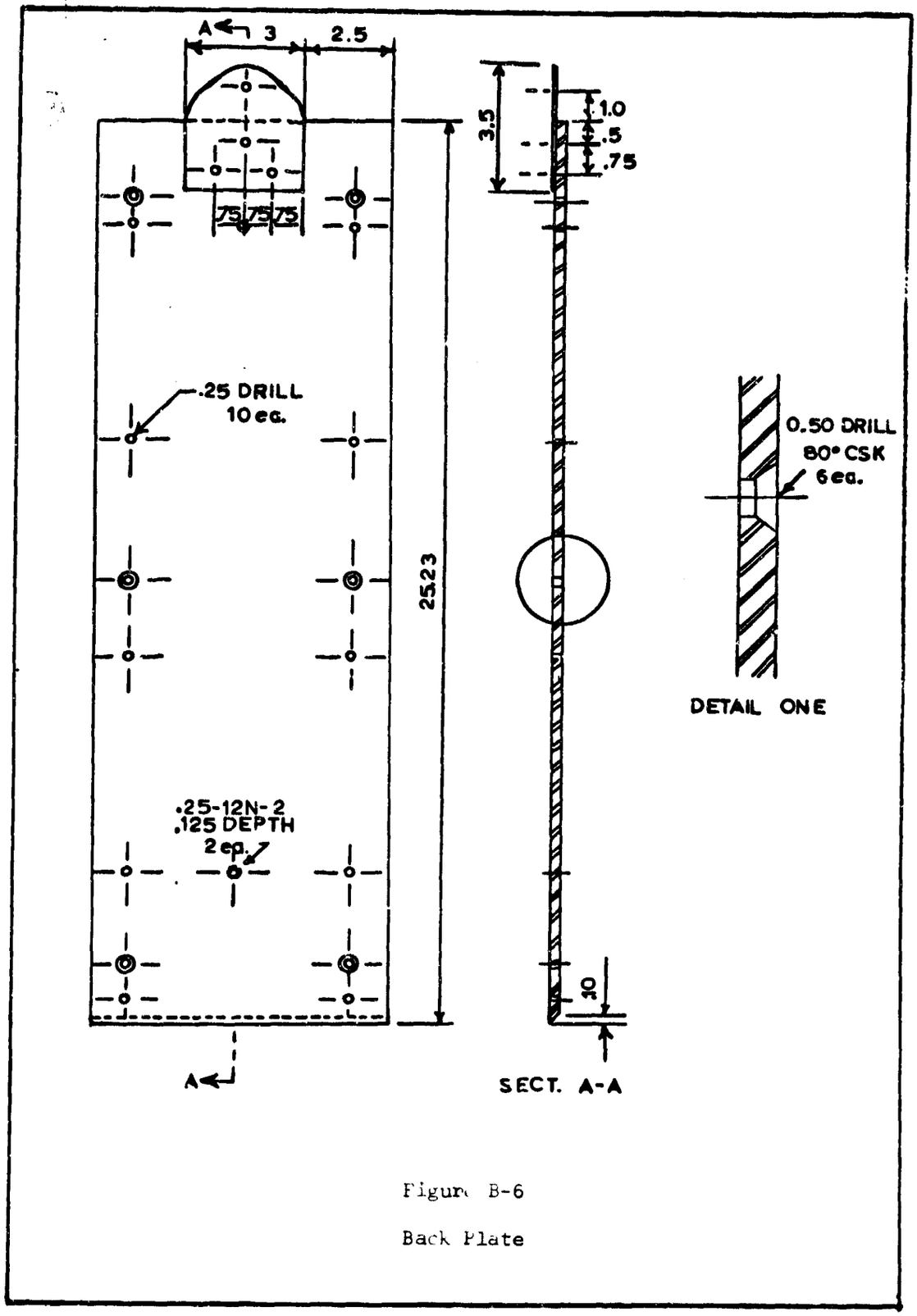

Figure B-6

Back Plate

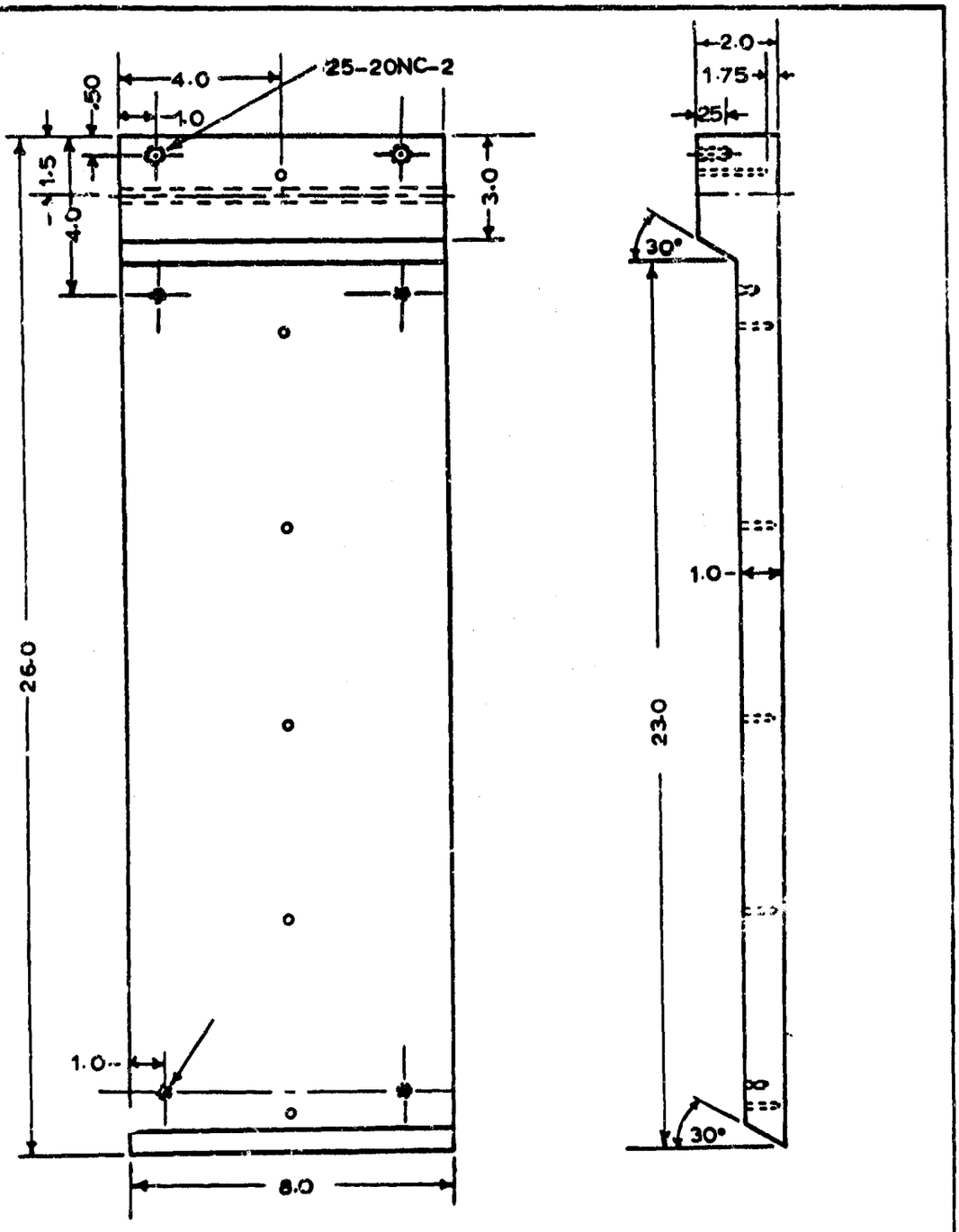

Figure B-7

Heating Plate

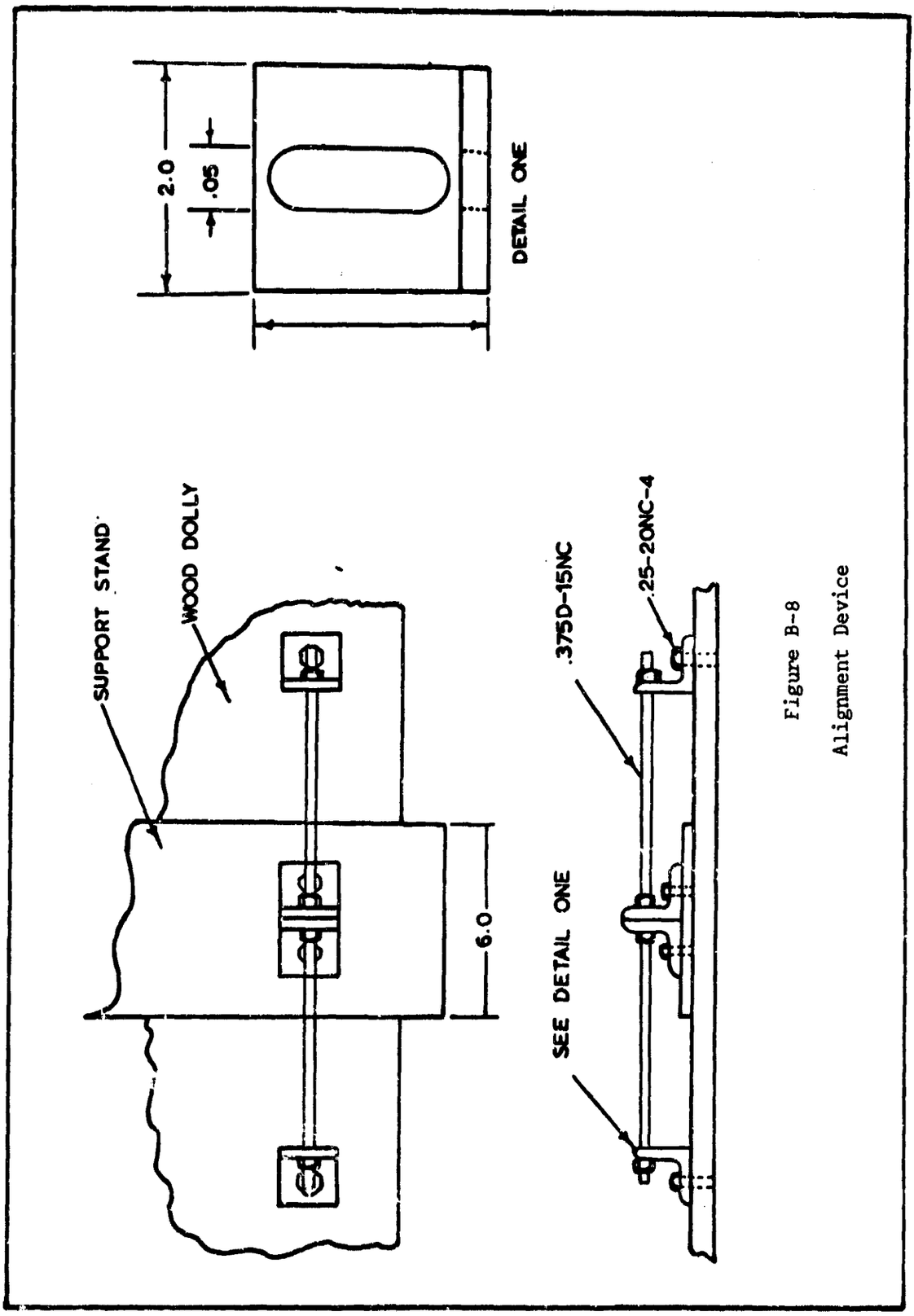

Figure B-8

Alignment Device

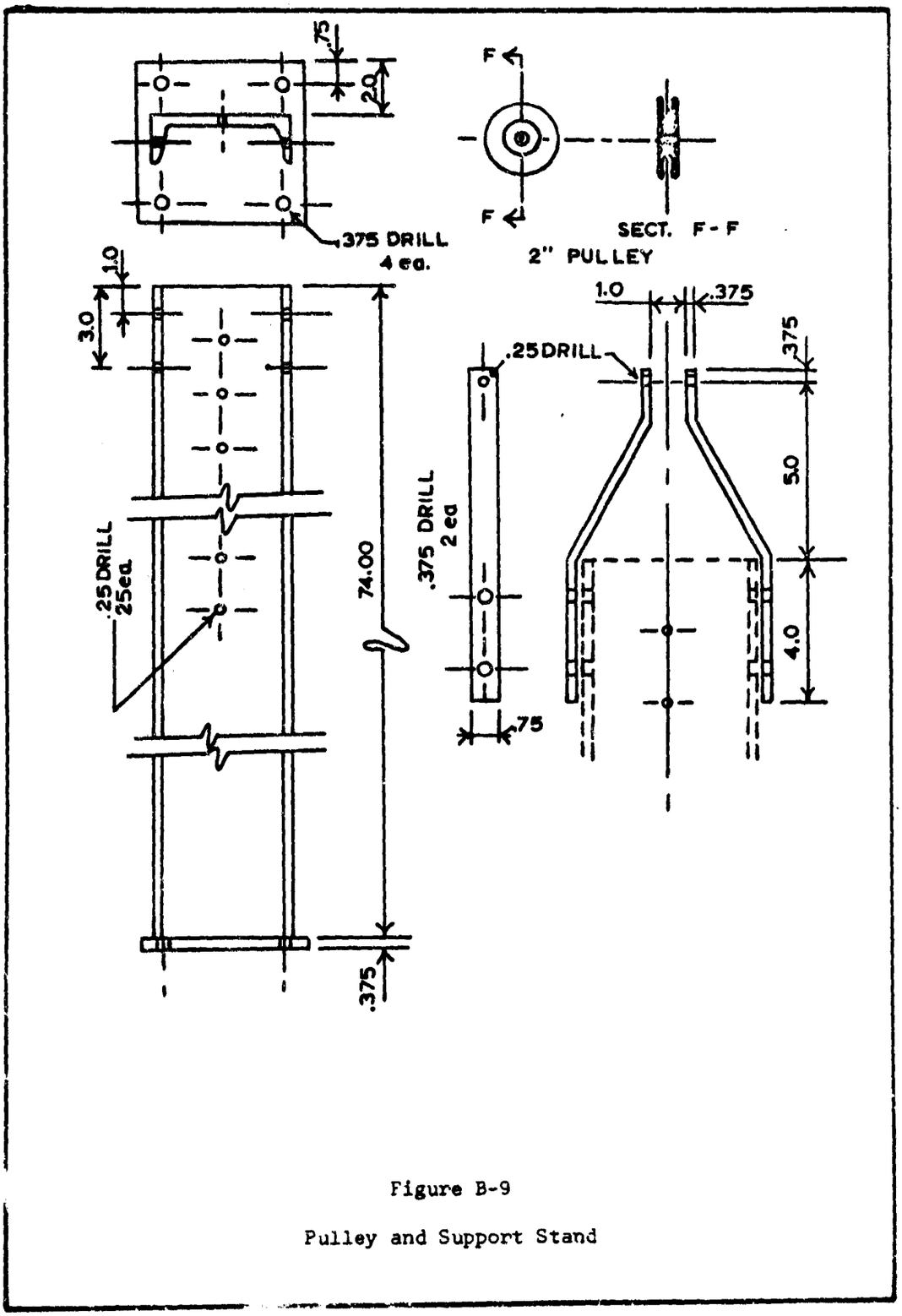

Figure B-9

Pulley and Support Stand

Appendix C

Cavity Alignment Procedures

A precision alignment method was needed to ensure that the first three fringes could be observed in the interferograms. The method which was chosen consisted of "butting" a 0.019 in diameter wire against the plate surface (at room temperature) and observing the point of contact. If the plate surface and the interferometer light rays were not parallel, part of the wire would appear to enter the plate surface. By placing this wire on both sides of the plate and observing the photographs (Fig C-2), it could be determined in which direction the plate needed to be rotated about the X axis. This adjustment was accomplished by using the alignment device (Fig B-8). This process was repeated using a smaller wire (0.005 in diameter) to make finer adjustments.

The plate was then heated to the desired temperature. The next step was to adjust the test stand so that the plate surface was perpendicular to the floor. A carpenter's level was used to check this condition. The final step in aligning the cavity was to align the expansion and recompression walls with the interferometer light rays. It was found that this could best be accomplished by observing the first fringe. When it was visible throughout the cavity, this final adjustment (rotation about the Y axis) completed the alignment procedure.

Figure C-2 is a series of photographs illustrating the alignment procedure. Photographs a thru c show the 0.019 in wire being used to make the rough adjustment about the X axis. In photograph a of this

figure, a bright white line can be observed on the plate surface. This is an indication that the plate was misaligned. The bright white line was caused by the light rays hitting the surface at an angle and reflecting off the surface, thus intensifying the light that passes the area near the plate surface. Photographs d thru f illustrate the same procedure being repeated with the 0.005 in wire. Photograph g was taken after the vertical adjustment was completed. In photograph h of this series, the bright line appears on the expansion wall and the first fringe cannot be seen throughout the cavity. Both indicate that the cavity walls are not aligned. After the final adjustment (rotation about the Y axis) was made, the final photograph i illustrating a properly aligned cavity was taken.

By measuring the visible part of the wire at the contact point, it was determined that this alignment procedure allowed only 0.002 in from the plate surface to be hidden and most of this was caused by a schlieren effect. This was well within the desired accuracy.

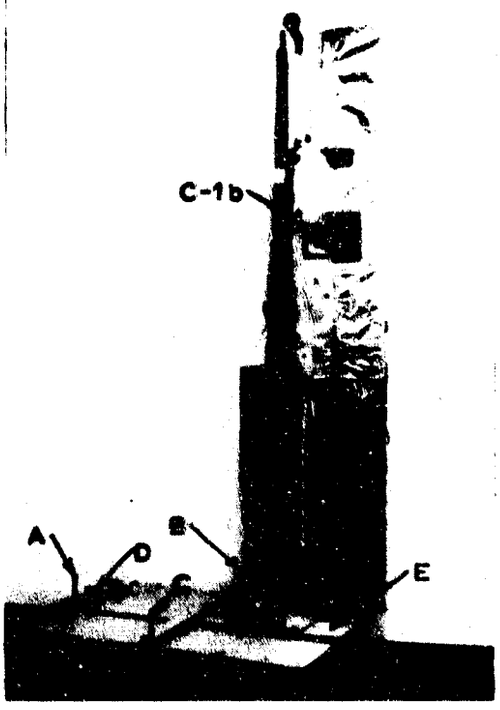

Figure C-1a

Cavity Alignment Nomenclature

A Vertical alignment bolt

B Horizontal alignment bolt

C Horizontal alignment bolt

D Alignment device
(for rotation about X axis)

E Pivot Point

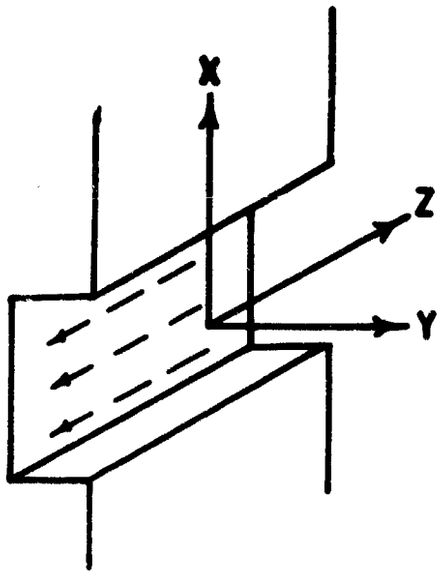

Figure C-1b
Cavity Coordinates

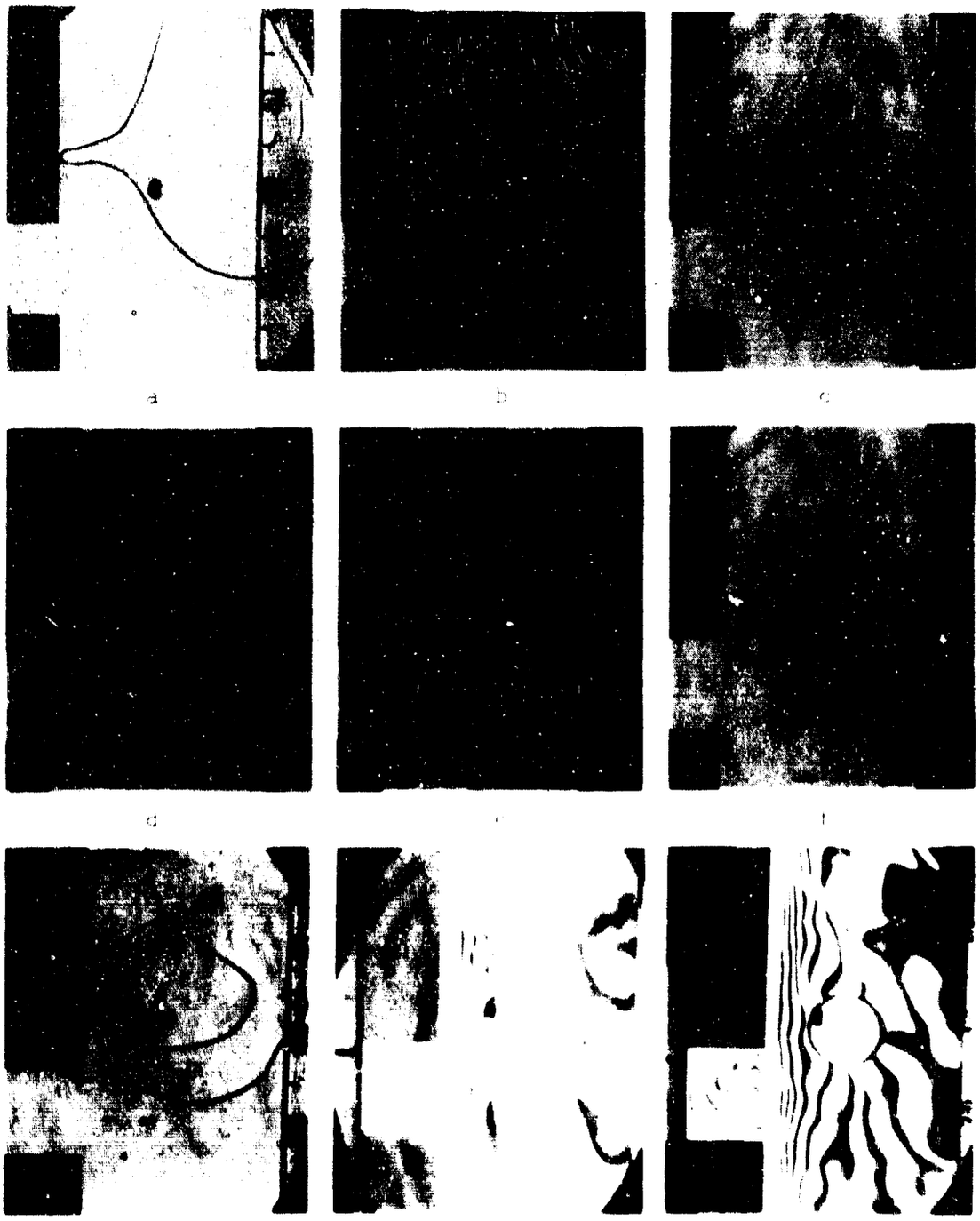

Figure C-2
Cavity Alignment Sequence

Appendix D

Computer Program

Figure D-1 is the computer source program which was developed to aid in the data reduction. The program was run on an IBM 1620 digital computer and the language used is Fortran II. The temperature gradient at the plate surface was approximated by averaging the temperature gradient between the first two pairs of fringes. The following is a list of the program variables and their meanings.

RHOW	Density of reference area	(lb_m/ft^3)
RHO1	Density of first fringe	(lb_m/ft^3)
RHO2	Density of second fringe	(lb_m/ft^3)
RHO3	Density of third fringe	(lb_m/ft^3)
T1	Temperature of first fringe	(R)
T2	Temperature of second fringe	(R)
T3	Temperature of third fringe	(R)
DELT1	Temperature difference between first and second fringe	(R)
DELT2	Temperature difference between second and third fringe	(R)
SY1	Actual distance between first and second fringe	(ft)
SY2	Actual distance between second and third fringe	(ft)
GRAD1	Temperature gradient between the first and second fringe	(R/ft)
GRAD2	Temperature gradient between the second and third fringe	(R/ft)
AGRAD	Average temperature gradient	(R/ft)

H(I)	Coefficient of convection heat transfer	(BTU/hr ft^2 R)
GR	Grashof number	
CNU	Nusselt number	

A set of input data consisted of one card with the following information:

X1	Elevation or distance from leading edge of the first station	(in)
XW1R	Photographed length of reference wire	(in)
BP	Barometric pressure	(in of mercury)
N	Number of stations being measured	
TW	Temperature of the wall	(R)
TA	Ambient temperature	(R)

followed by N cards with the following information:

Y1(I)	Coordinate of the first fringe	(in)
Y2(I)	Coordinate of the second fringe	(in)
Y3(I)	Coordinate of the third fringe	(in)
X	Elevation of particular station	(in)

A set of data cards was necessary for each interferogram analyzed.

Figure D-2 is a sample of the computer print-out for a single interferogram and Fig D-3 is a print-out of a simple averaging program which averaged the results of four interferograms.

```
C  C  INTERFEROMETER  STUDY  LT. KARL  LUESSE  GAM  69-10
      DIMENSION SY1(35),SY2(35), H(35), B(35),Y1(25),Y2(35),Y3(35)
      DIMENSIONGRAD1(35),GRAD2(35),AVGD(35)
      M=0
    1 READ,XL,XWIR,BP,N,TW,TA
      TW=0.0
      DELTO=TW-TA
      RHOW=(BP*70.73)/(53.34*TW)
      PUNCH 101,TA,TW
  101 FORMAT(/,13HAMBIENT TEMP=,F6.2,5X,11HPLATE TEMP=,F6.2)
      PUNCH 105
  105 FORMAT( /,8HPOSITION,2X,13HAVERAGE DT/DY,3X,1HH,7X,11HGRASHOF NO.,
     17X,11HNUSSELT NO.,/)
      DO7 I=1,M
      READ,Y1(I),Y2(I),Y3(I),X
      B(I)=1.0
      RHO3=RHOW+0.000766*(2.5+(B(I)-1.0))
      RHO2=RHOW+0.000766*(1.5+(B(I)-1.0))
      RHO1=RHOW+0.000766*(0.5+(B(I)-1.0))
      T1=(BP*70.73)/(RHO1*53.34)
      T2=(BP*70.73)/(RHO2*53.34)
      T3=(BP*70.73)/(RHO3*53.34)
      DELT1=T2-T1
      DELT2=T3-T2
      SY1(I)=(3.001*(Y2(I)-Y1(I)))/XWIR
      SY2(I)=(3.001*(Y3(I)-Y2(I)))/XWIR
      GRAD1(I)=12.0*DELT1/SY1(I)
      GRAD2(I)=12.0*DELT2/SY2(I)
      AVGD(I)=0.5*(GRAD1(I)+GRAD2(I))
      H(I)=0.01758*AVGD(I)/DELTO
      GR=(1396000.0/1728.0)*DELTO*(X**3)
      CNU=(H(I)*X)/(0.01758*12.0)
      TW=TW+H(I)
      PUNCH 103,X,AVGD(I),H(I),GR,CNU
  103 FORMAT(/,F6.3,5X,F9.2,2X,F9.4,2X,1PE16.6,2X,1PE16.6)
    7 CONTINUE
      ATH=TW/20.0
      PUNCH 104,ATH
  104 FORMAT(/,45HAVERAGE CONVECTIVE HEAT TRANSFER COEFFICIENT=,F9.4)
      M=M+1
      IF(M-4)1,99,99
   99 STOP
      END
```

Figure D-1

Computer Source Program

C C INTERFEROMETER STUDY LT. KARL LUESSE GAM 69-10

AMBIENT TEMP=532.00 PLATE TEMP=662.00

POSITION	AVERAGE DT/DY	H	GRASHOF NO.	NUSSELT NO.
44.200	7019.94	.9493	9.068842E+09	1.988983E+02
44.450	6889.25	.9316	9.223597E+09	1.962995E+02
44.575	7394.41	1.0000	9.301631E+09	2.112857E+02
45.825	7947.96	1.0748	1.010631E+10	2.334712E+02
45.950	6709.15	.9073	1.018924E+10	1.976188E+02
46.200	6216.74	.8407	1.035645E+10	1.841111E+02
46.450	5568.11	.7530	1.052549E+10	1.657940E+02
46.700	5399.43	.7302	1.069635E+10	1.616369E+02

Figure D-2

Sample Computer Print-Out for a Single Interferogram

POSITION	AVERAGE H	AVERAGE GRASHOF NO.	AVERAGE NUSSELT NO.
44.200	.8868	9.068842E+09	1.857919E+02
44.450	.8859	9.223597E+09	1.866513E+02
44.575	.9038	9.301631E+09	1.909574E+02
45.825	1.3506	1.010631E+10	2.933662E+02
45.950	1.2745	1.018924E+10	2.776016E+02
46.200	.9540	1.035645E+10	2.089207E+02
46.450	.9328	1.052549E+10	2.053778E+02
46.700	.9059	1.069635E+10	2.005336E+02

Figure D-3

Sample Computer Print-Out of Averaging Program

Vita

Karl Edward Luesse was born on 24 April 1942 in Greenwich, Connecticut, the son of Karl Henry Luesse and Leda Marie Luesse. After completing his work at Port Chester Senior High School, Port Chester, New York, in 1960 he entered Westchester Community College, Valhalla, New York. He received an Associate in Applied Science degree in 1962. In an effort to complete his education he enrolled at the University of Bridgeport, Bridgeport, Connecticut. He enlisted in the U.S. Air Force in 1963. After serving two years at Andrews AFB, Washington, D.C., as a jet aircraft mechanic, he was accepted in the Airmen's Education and Commissioning Program (AECP). On 17 March 1967 he received a Bachelor of Mechanical Engineering degree from Auburn University, Auburn, Alabama. He was commissioned in San Antonio on 27 May 1967 and was assigned to the Air Force Institute of Technology, Wright-Patterson Air Force Base, Ohio.

Permanent address: 1 Brook Road
Port Chester, New York

This thesis was typed by Mrs. Imogene J. Hoffer.

UNCLASSIFIED
Security Classification

DOCUMENT CONTROL DATA - R & D

(Security classification of title, body of abstract and indexing annotation must be entered when the overall report is classified)

ORIGINATING ACTIVITY (Corporate author)	2a. REPORT SECURITY CLASSIFICATION
Air Force Institute of Technology (AFIT-SE) Wright-Patterson Air Force Base, Ohio 45433	Unclassified
	2b. GROUP

3. REPORT TITLE

Interferometer Study of Free Convection About a Rectangular Cavity in a Flat Plate

4. DESCRIPTIVE NOTES *(Type of report and inclusive dates)*

AFIT Thesis

5. AUTHOR(S) *(First name, middle initial, last name)*

Karl E. Luesse
1/Lt USAF

6. REPORT DATE	7a. TOTAL NO. OF PAGES	7b. NO. OF REFS
March 1969	55	13

8a. CONTRACT OR GRANT NO.	9a. ORIGINATOR'S REPORT NUMBER(S)
b. PROJECT NO.	GAM/ME/69-10
c. N/A	9b. OTHER REPORT NO(S) *(Any other numbers that may be assigned this report)*
d.	

10. DISTRIBUTION STATEMENT This document is subject to special export controls and each transmittal to foreign government or foreign nationals may be made only with prior approval of the Dean of Engineering, Air Force Institute of Technology (AFIT-SE), Wright-Patterson Air Force Base, Ohio 45433.

11. SUPPLEMENTARY NOTES	12. SPONSORING MILITARY ACTIVITY

13. ABSTRACT

Interferometer study to determine the effect of a rectangular cavity on the heat transfer rate from a heated vertical flat plate. Cavities 1 in wide with depths of 0.2 in, 0.4 in and 0.6 in was placed perpendicular to the flow. Each cavity was located at four elevations 26.7 in, 32.7 in, 38.7 in and 44.7 in. The temperature difference was constant at 130 R which resulted in a Grashof number range of 1.75×10^9 to 1.24×10^{10}. The flow over the smooth flat plate went from laminar to turbulent. The cavity's effect was dependent on the type of flow. The heat transfer rate was increased in the laminar regime and decreased in the turbulent regime.

DD FORM 1 NOV 65 1473

UNCLASSIFIED
Security Classification

14. KEY WORDS	LINK A		LINK B		LINK C	
	ROLE	WT	ROLE	WT	ROLE	WT
Interferometer						
Free Convection						
Turbulent						
Rectangular Cavity						